COVALENTLY BOUND REDOX DYES AS POTENTIAL ELECTRON MEDIATORS IN HYDROGEN PEROXIDE AND GLUCOSE BIOSENSORS

A dissertation submitted for the degree of
DOCTOR OF PHILOSOPHY

by

B S B SALOMI

Department of Biochemistry
School of Life Sciences
University of Hyderabad
Hyderabad, India

March 2006
Enrollment No. 02LBPH01

Dedicated to my
parents and sister

UNIVERSITY OF HYDERABAD
Department of Biochemistry
School of Life Sciences

Certificate

This is to certify that the thesis entitled ***"Covalently bound redox dyes as potential electron mediators in hydrogen peroxide and glucose biosensors"*** *is based on the research work carried out by Ms. B S B Salomi in fulfillment for the Degree of Doctor of Philosophy under my supervision. This work has not been submitted for any degree or diploma to any other university.*

Chanchal K Mitra
(Supervisor)

Head
(Dept of Biochemistry)

Dean
(School of Life Sciences)

UNIVERSITY OF HYDERABAD
Department of Biochemistry
School of Life Sciences

Declaration

*I hereby declare that the work presented in this thesis entitled **"Covalently bound redox dyes as potential electron mediators in hydrogen peroxide and glucose biosensors"** has been carried out by me under the supervision of Prof. Chanchal K Mitra and that this work has not been submitted for a degree or diploma at any other university.*

Date: B S B Salomi

(Enrollment No. 02LBPH01)

ACKNOWLEDGEMENTS

It is my joy to thank the innumerable persons without whose help and advice this venture wouldn't have been possible.

It gives me immense pleasure to express my profound gratitude and deep respect to my supervisor, Prof. Chanchal K Mitra for his constant inspiration and valuable thought-provoking discussions.

My indebtedness and sincere respects are due to Prof. Lo Gorton for his guidance and hospitality during my stay in Sweden. I am fortunate for his discussions.

I thank the Dean, School of Life Sciences, Head, Department of Biochemistry and all the faculty members of the School for their help and cooperation during my research.

I thank all the non-teaching staff of the School of Life Sciences, staff members of CMSD and CIL, for their assistance on various occasions.

I wish to record my thanks to UPE (University of Hyderabad), SIDA (Swedish International Development Cooperation Agency) and VR (Swedish Research Council) for the financial assistance.

I wish to thank my friendly and cooperative labmates Ashok, Shashi Rekha, Goutham, Sridevi, Ramesh and my previous labmates Dr. Pavan, Dr. Shailly Varma, Dr. Anitha, and Venu for creating a cheerful work atmosphere.

It is impossible to mention the names of every single person to whom I am indebted; nevertheless I would like to mention with appreciation the names of some who made my stay in this campus pleasant. They include (alphabetically) Florence, Haritha, Jayasri, Kalyani, Lavanya, Nageshwari, Neeraja, Pushpa, Riaz, Roda, Sailaja, Sirisha, Sirisha (Eng. Dept), Sneha and Sudar.

I cannot forget to acknowledge the love and prayers of my relatives and family friends whose list is very vast. I would however like to express my gratitude to my Grandmother Gnana Bhushanam for her constant prayers. The support and love of my aunt Late. Dr. Jayaprada is greatly acknowledged.

Words cannot express my gratitude to my beloved Dad and Mom for their constant support and encouragement with their love and prayers. A special note of thanks to my sister Annie and my brother-in-law John who supported me through this ordeal. The little pranks of my niece Lydia kept me lively.

Above all, I owe my gratitude to the LORD ALMIGHTY for his blessings and *all-sufficient grace*.

TABLE OF CONTENTS

ABBREVIATIONS

ACV	Alternate Current Voltammetry
BSA	Bovine Serum Albumin
BCB	Brilliant cresyl blue
CV	Cyclic Voltammetry
DCC	dicyclohexylcarbodiimide
DPV	Differential Pulse Voltammetry
EDC	1–ethyl–3–(3–dimethyl aminopropyl) carbodiimide hydrochloride
FIA	Flow Injection Analysis
GA	Glutaraldehyde
GOx	Glucose oxidase
HRP	Horseradish Peroxidase
mV	millivolts
nA	nanoampere
NB	Nile blue A
nm	nanometer
NR	Neutral red
PEGDGE	Poly(ethylene glycol) 400 diglycidylether
SF	Safranine O
TB	Toluidine blue
μA	microampere

INTRODUCTION

1 INTRODUCTION

1.1 GENERAL ASPECTS

The selective and sensitive determination of a particular analyte is of great interest in the field of science and technology. There has been considerable progress in modern analytical instrumentation. To broaden the field of sensing and for rapid determination, biosensors, which are highly selective, sensitive and easy to handle, have been developed.

The specificity and sensitivity of biological receptors such as enzymes and antibodies make them highly attractive for development of various sensors for chemical and biochemical species, which led to the development of biosensors.

1.2 BIOSENSORS

A biosensor can be defined as a device incorporating a biological sensing element either intimately connected to, or integrated within a transducer.[1-3] The biological sensing element can be either enzymes, receptors, antigens, antibodies, hormones, nucleic acids, membranes, organelles, cells, tissues, or organism. The transducers can be either electrochemical, thermal, optical, acoustic or mechanical.

Fig. 1.1 shows the block diagram of a biosensor. In presence of the analyte, the biological sensing element senses the analyte by binding with the analyte. This binding is recognized by a transducer, which produces a signal, mostly an electrical signal (at times optical and other signals). The signal is later processed, amplified and given out as a meaningful output.

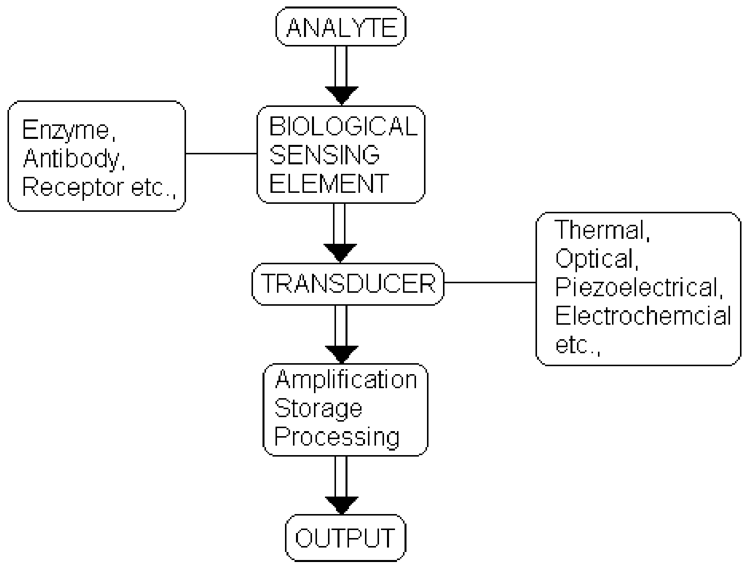

Figure 1.1: Block diagram showing the information flow through the components of a biosensor

1.2.1 Biological sensing element

Selectivity or specificity is the ability of a sensor to respond to one species in presence of similar or analogous species. This is achieved by using highly selective biological elements such as enzymes, antigens, hormones, etc., that show affinity for their complementary structures such as substrates, antibodies, receptors, etc., respectively. The biological element senses the complementary structure by its binding to the sensing element. The complementary structure is not sensed in the absence of its binding to the biological element. The binding of the analyte with the biological sensing element is recognized by a transducer, which in turn produces a meaningful signal.

Since the binding of the analyte to the biological element usually produces a very small change, immobilizing the biological sensing element onto the transducer increases the efficiency of the output. The techniques for immobilizing biological sensing elements comprise of physical and chemical methods as well as combinations of both.[4,5]

1.2.1.1 Adsorption

It is the simplest method of immobilization. It is based on the adhesion of the biomolecules on the surface of a solid matrix. The major forces responsible for binding may be hydrogen bonding, van der Waals interaction, etc. In addition to the simplicity of the procedure, the advantage of adsorptive immobilization is that it does not need non-physiological coupling conditions or chemicals potentially impairing enzyme or cell functions. An activity loss is therefore seldom observed.[6] Since the binding of the biological element is only physical, and therefore a week interaction, leaching of the adsorbed substance into the solution is often observed which is the main disadvantage of this method.[7]

1.2.1.2 Gel Entrapment

In this method the biomolecules are entrapped in a matrix formed by organic polymers. Entrapment in polymeric gels prevents the biomolecules from diffusing, and on the other hand, small substrate and effector molecules can easily permeate through them. Except for the use of strong chemicals during the formation of the gels, which may impair the function of the biological elements, gel entrapment is as mild a procedure as adsorption.

1.2.1.3 Covalent coupling

It is based on the covalent (sharing of electrons between the biomolecules and the matrix) attachment of the biomolecules on the surface of a water insoluble support. In this case the matrix needs to be functionalized or activated. It is an efficient method of immobilization as the bonding is strong and the biomolecules are not lost in the solution. The reaction should involve only groups that are not essential for the biological activity of the biomolecules. A disadvantage of covalent coupling is the frequent loss of activity.

1.2.1.4 Cross-linking

The biomolecules may be cross-linked with each other or with another functionally inert protein. The bio-macromolecules can also be adsorbed to a water-insoluble carrier or entrapped in a gel and then cross-linked. The advantages of cross-linking are its simple procedure and the strong chemical binding of the biomolecules. The main drawback is the possibility of activity-loss due to chemical alterations of the catalytically essential sites of the protein.

1.2.2 Transducers

The physiochemical change of the biological sensing element resulting from the interaction with the analyte is converted into a measurable meaningful output, mostly an electrical signal, by an appropriate transducer. Performance factors like sensitivity range, accuracy and response time, which depend on the type of transducer, contribute to the efficiency of the biosensor. The transducers can be electrochemical, thermal, optical, or mechanical.

1.2.2.1 Thermal transducers

All chemical processes exhibit enthalpy change. This can be measured by sensitive thermistors and can be related to the amount of reaction. The main advantage of the thermal transducers is its broad universal applicability.

Because the enthalpy changes observed are very small for the biological reactions, highly sensitive thermistors have to be used. Since thermistors existing today cannot measure a temperature change of $<10^{-3}$ °C, it limits the applications of thermal transducers.

1.2.2.2 Optical transducers

Optical transducers detect the changes in optical properties like absorption, fluorescence, chemiluminescence, refraction, phosphorescence, etc. Most of these transducers comprise of a light source, optical fiber and an appropriate optical detector. Fig. 1.2 shows the light transmission in an optical transducer. Optical sensors have several advantages of which the absence of their susceptibility to disturbances by electric fields is the main advantage.

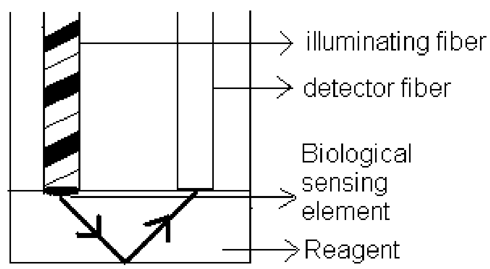

Figure 1.2: Light transmission in optical transducer. The enzyme is entrapped or immobilized in the reagent layer most often at the tip of the fiber.

1.2.2.3 Piezoelectric transducers

The principle of this sensor is that the frequency of vibration of an oscillating crystal (anisotropic crystals such as quartz) is decreased by the adsorption of a foreign material on its surface. The crystal is sensitized by covering it with the biological element that reacts with the analyte to be determined.[8] Added to the very minute changes in the frequency of vibration upon the analyte binding to the sensing element needing a highly sensitive device to recognize the signal and the difficulty for the adaptation of this technique to aqueous systems, i.e., to the conditions common for biological systems are the disadvantages of these transducers.

1.2.2.4 Electrochemical transducers

Electrochemical transducers have practical advantages such as operational simplicity, low cost of fabrication and real-time detection. They prevail over all other methods of transduction. They use electrodes as the transduction elements, which are connected internally through an electrolyte and externally through a conductor. These transducers can operate potentiometrically or amperometrically.

1.2.2.4.1 Potentiometric sensors

The simplest potentiometric technique is based on the concentration dependence of the potential, *E*, at reversible redox electrodes according to the Nernst equation,

$$E = E_0 + \frac{RT}{nF} \log_e \frac{[Ox]}{[Red]} \tag{1.1}$$

where E_0 is the standard redox potential, *R* is the gas constant, *T* is absolute temperature, *F* is Faraday constant, *n* is the number of electrons involved in the redox reaction, [*Ox*], the concentration of the oxidized form and [*Red*], the concentration of the reduced form of the substance. Examples of potentiometric sensors include sensors using ion selective electrodes and silicon based sensors.[9,10]

1.2.2.4.2 Amperometric sensors

Amperometric sensors are based on the heterogeneous electron transfer reactions, i e., oxidation and reduction of electro-active substances at a potential.[11] By increasing the over-voltage, i.e., deviation from the redox potential, the electron transfer can be enhanced and the whole process is controlled by the mass transfer. Under these conditions the current is proportional to the concentration of the analyte given by the equation,

$$I = nAFD\left(\frac{dc}{dx}\right)_{x=0} \tag{1.2}$$

where I is current in amperes, n is the number of electrons transferred, A is the electrode area, F is Faraday constant, D is the diffusion coefficient and dc/dx is the flux of C (electroactive species) at the electrode surface. Detection limits as low as 10 nM concentration and a linear measuring range are the main advantages of amperometric techniques.

1.2.3 Types of biosensors

Based on the degree of intimacy between the biocatalyst and the transducer, biosensors are categorised as first, second and third-generation instruments.[12]

1.2.3.1 First-generation biosensors

A first generation biosensor is where the normal product of the reaction diffuses to the transducer and causes the response.

1.2.3.2 Second-generation biosensors

These involve specific 'mediators' between the reaction and the transducer in order to generate improved response. It was observed that these mediators could efficiently decrease the applied potential of the biosensors,[13] and thereby decrease the interference from electrochemically oxidisable compounds present in the sample.

1.2.3.3 Third-generation biosensors

Third generation biosensors are where the reaction itself causes the response and no product or mediator diffusion is directly involved. They involve the most intimate interactions of the biocatalyst and transducer with direct electron transfer between them. Early studies demonstrated, that certain enzymes or redox proteins can exhibit electrical communication with electrode supports, and that electrically-stimulated biocatalytic transformations can be driven by that process.[14]

1.3 ELECTROCHEMISTRY

1.3.1 Definition

Electrochemistry is the study of reactions in which charged particles (ions or electrons) cross the interface between two phases of matter, typically a metallic phase (electrode) and a conductive solution or electrolyte.

1.3.2 Electrochemical cell

An electrochemical cell consists of minimum two electrodes connected internally through an electrolyte and externally through a conductor. Each electrode-solution interface constitutes an oxidation-reduction half-cell; associated with it is an electrode-solution potential difference whose magnitude depends on the nature of the particular electrode reaction and on the concentrations of the electro-active species. Fig. 1.3 shows a typical 3-electrode setup consisting of a working electrode, reference electrode and a counter electrode.

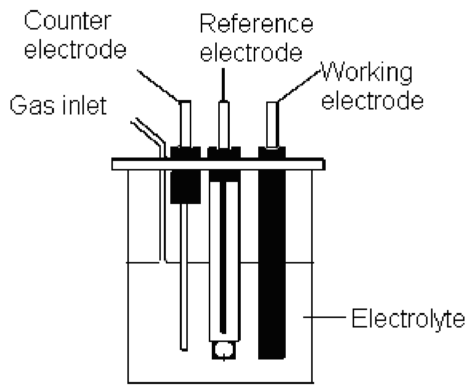

Figure 1.3: A typical 3-electrode setup consisting of a working electrode, a reference electrode and a counter electrode.

Working electrode: It acts as a source or sink of electrons for exchange with molecules in the interfacial region where the electrochemistry of interest takes place. It must be an electronic conductor and preferably be electrochemically inert i.e., does not generate a current in response to an applied potential over a wide potential range. Commonly used working electrode materials include platinum, gold, mercury, graphite and glassy carbon. Other materials like semiconductors are also used, for more specific applications. The choice of material depends upon the potential window required (e.g., mercury can only be used for negative potentials, due to oxidation of mercury at more positive potentials), as well as the rate of electron transfer (slow electron transfer kinetics can affect the reversibility of redox behavior of the system under study). The rate of electron transfer can vary considerably from one material to another, even for the same analyte, due to, for example, catalytic interactions between the analyte and active species on the electrode surface.

Reference electrode: Since the potential of a given electrode can only be measured relative to another electrode a reference electrode is used to measure the potential of the working electrode.[15] An ideal reference electrode should exhibit a constant potential with change in time. Table 1.1 shows the standard potentials of commonly used reference electrodes.

Table 1.1: Potentials of standard reference electrodes

Reference electrode		Potential (V vs. SHE)
Standard Hydrogen Electrode (SHE)		0.00
Silver chloride	0.1 M KCl	0.2881
	saturated (KCl)	0.199
Calomel	0.1 M KCl	0.3337
	saturated (KCl)	0.241

Counter electrode: It provides a surface for a redox reaction to balance the one occurring at the surface of the working electrode. In order to support the current generated at the working electrode, the surface area of the auxiliary electrode must be preferably equal to, or larger than that of the working electrode. A platinum wire is widely used for this purpose.

Electrochemical cells are divided into two groups

(i) Galvanic cells - A galvanic cell is one in which reactions occur spontaneously at the electrodes when they are connected externally by a conductor. Potentiometry is a technique, which involves the use of galvanic cells.

(ii) Electrolytic cells – An electrolytic cell is one in which reactions are effected by the imposition of an external voltage to the electrode greater than the spontaneous potential of a cell. Voltammetry is a technique, which involves the use of electrolytic cells.

1.3.3 Voltammetric techniques

Voltammetric techniques involve reactions effected by an imposed external voltage greater than the spontaneous potential of the cell. The reactions occurring within the cell can be considered as reactions occurring at the surface of an electrode in which the electrode supplies electrons (reduction) or removes electrons (oxidation).

For instance, consider a half-cell containing a solution of an electro-reducible species. As the potential of the electrode is made progressively more negative, a point will be reached when the reduction of the species will begin at the electrode and a small current will flow. As the potential is made even more negative, the current will increase as more reduction of the species occurs, until a potential is reached where the species is reduced at the electrode surface as quickly as it is able to reach the electrode surface by diffusion. At this point the maximum or limiting current is achieved, and further increase in the potential will not affect the current.

The resulting plot of current (Fig. 1.4) against voltage has two important properties.

(i) The midpoint of the wave (called the half-wave potential) is characteristic for each species being reduced.

(ii) Since the magnitude of the limiting current is controlled by the rate of diffusion of the reducible species, it will be directly proportional to the concentration of this species.

These features enable voltammetric techniques to be used both to identify and to quantify electro-active materials in solution. Voltammetric techniques are of two types: amperometry and voltammetry or polarography.

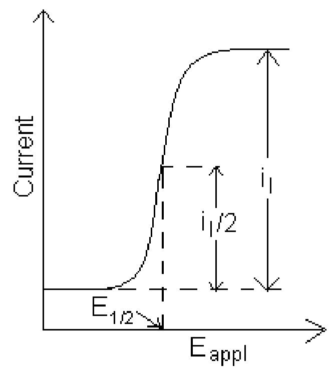

Figure 1.4: An idealized plot showing the resultant current as applied potential is increased linearly with time. E_{appl} represents the applied potential, $E_{1/2}$ represents the half-wave potential, i_l the limiting current and i_l / 2 the current at half-wave potential.

1.3.3.1 Amperometry

It is the measurement of the current passing through the electrode at constant potential. It involves the reduction or oxidation of electro-active species, usually at the limiting current, such that the mass transfer controls the whole process. Under these conditions the current I is proportional to the concentration of the species of interest given by Eq. 1.2

Detection limits as low as 10 nM concentration and a linear measuring range of 3-6 concentration decades are the main advantages of amperometric techniques.

1.3.3.2 Voltammetry / Polarography

It is the measurement of the current while the potential varies under a potentiostatic control. There are various types of voltammetric techniques based on the type of excitation signal (variation of potential with time) as shown in Fig. 1.5.

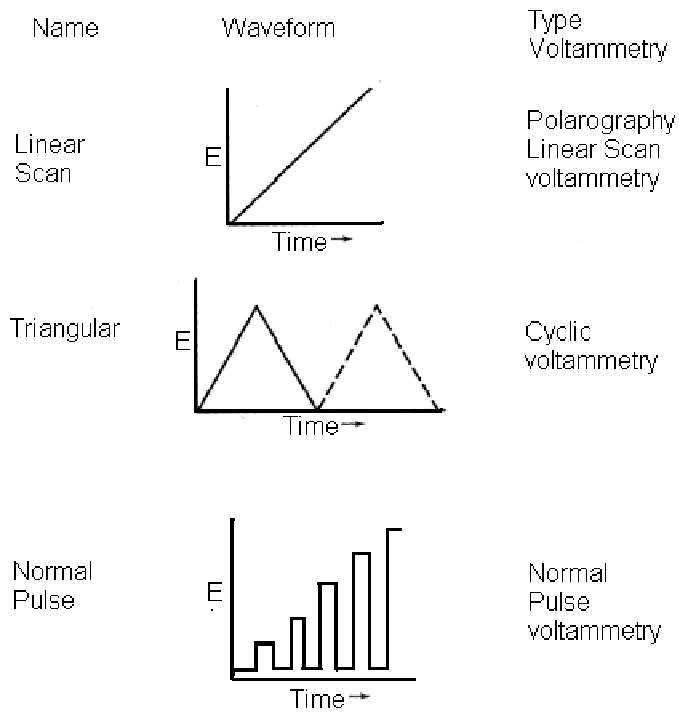

Figure 1.5: Various types of voltammetry based on excitation signal. The excitation signal is the variation of potential E with time.

1.3.3.2.1 Linear scan voltammetry (LSV)

The excitation signal i.e., potential applied in LSV varies linearly with time at a certain rate.

1.3.3.2.2 Cyclic voltammetry (CV) [16]

The excitation signal for a CV is a linear scan with triangular waveform. The potential applied at the electrode is varied from an initial value to a final value (forward scan) after which the sweep direction is changed to the initial value (reverse scan).

Fig. 1.6 shows a typical cyclic voltammogram. The potential scan is started at a potential away from the redox potential of the analyte so that there is no net conversion of the reduced form (R) to oxidized form (O). As the redox potential is approached, there is a net anodic current, which increases with potential. As R is converted into O, concentration gradients are set up for both R and O, and diffusion occurs down these concentration gradients. At the anodic peak, the redox potential is sufficiently positive that any R that reaches the electrode surface is instantaneously oxidized to O. Therefore, the current now depends upon the rate of mass transfer to the electrode surface and so the time dependence is qt resulting in an asymmetric peak shape. Upon reversal of the scan the current continues to decay with a qt until the potential nears the redox potential. At this point, a net reduction of O to R occurs which causes a cathodic current, which eventually produces a peak shaped response.

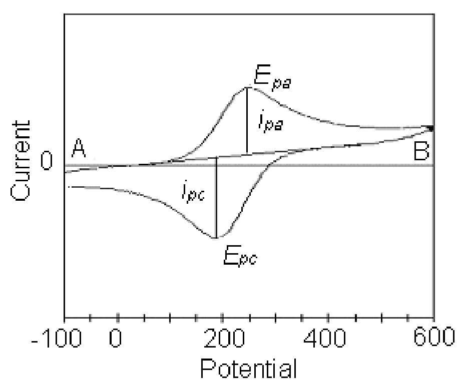

Figure 1.6: A typical cyclic voltammogram. The initial scan is from A to B and the reverse scan from B to A. E_{pa} and E_{pc} represent the anodic and cathodic peak potentials respectively and i_{pa} and i_{pc} the anodic and cathodic peak currents respectively.

The important parameters in a cyclic voltammogram are the peak potentials (E_{pc}, E_{pa}) and peak currents (i_{pc}, i_{pa}) of the cathodic and anodic peaks, respectively. The peak separation (ΔE_p) and the relationship of the peak current (i_p) with scan rate can give an idea about the kinetics of the electron transfer.[17]

If the electron transfer process is fast compared with other processes (such as diffusion), the reaction is said to be electrochemically reversible, and the peak separation (ΔE_p) is given by,

$$\Delta E_p = \left| E_{pa} - E_{pc} \right| = 2.303\, RT / nF \tag{1.3}$$

where E_{pa} and E_{pc} represent the anodic and cathodic peak potentials respectively. R, T, n, and F have their usual meanings as defined in Eq. 1.1.

Thus, for a reversible redox reaction at 25 °C with n electrons, ΔE_p should be 0.0592/n V or about 60 mV for one electron. In practice this value is difficult to attain because of such factors as cell resistance. Irreversibility due to a slow electron transfer rate results in ΔE_p > 0.0592/n V, greater, say, than 70 mV for a one-electron reaction.

The formal redox potential ($E^{o'}$) for a reversible couple is given by,

$$E^{0'} = \frac{E_{pc} + E_{pa}}{2} \tag{1.4}$$

Formal potential is the measured potential of the half-cell when the ratio of the concentration of the oxidized and reduced species is unity, under specified conditions in terms of the electrolyte.

For a reversible reaction, the concentration is related to peak current by the Randles–Sevcik expression (at 25 °C) as follows:

$$i_p = 2.686 \times 10^5 n^{3/2} A c^0 D^{1/2} \nu^{1/2} \tag{1.5}$$

where i_p is the peak current in amps, A is the electrode area (cm^2), D is the diffusion coefficient (cm^2 s^{-1}), c^0 is the concentration in mol cm^{-3}, and ν is the scan rate in V s^{-1}.

For a species adsorbed on the electrode, the peak current and indeed the current at all the points on the wave, is proportional to the scan rate (ν) in contrast to $\nu^{1/2}$ dependence observed for Nernstian waves of diffusion species as,

$$i_p = \frac{n^2 F^2}{4RT} \Gamma A \nu \qquad (1.6)$$

where i_p is the peak current, A is the surface area, ν is the scan rate, Γ the coverage and n the number of electrons transferred during the redox reaction.

The anodic and cathodic are mirror images reflected across the potential axis. For an ideal Nernstian reaction under Langmuir isotherm conditions $E_{pa} = E_{pc}$ and the total width at half-height of either the cathodic or anodic wave ($E_{p,1/2}$) is given by[18]

$$\Delta E_{p,1/2} = 3.53 \frac{RT}{nF} \qquad (1.7)$$

The location of E_p with respect to $E^{o'}$ depends on the relative strength of adsorption of O (b_O) and R (b_R) given as

$$E_p = E^{o'} - \left(\frac{RT}{nF}\right) \ln\left(\frac{b_O}{b_R}\right) \qquad (1.8)$$

Cyclic voltammetry is a powerful tool for the determination of formal redox potentials, detection of chemical reactions that precede or follow the electrochemical reaction and evaluation of electron transfer kinetics.

1.3.3.2.3 Alternating Current Voltammetry (ACV)

In ac voltammetry small amplitude sinusoidal voltage (nominally 1 to 10 mV) with a frequency of 10 Hz to 100 kHz rides on a constant or slowly changing potential ramp (nominally 5mV/s).[19] The sinusoidal (dc) potential is essentially constant during any single cycle of the sine wave and can be considered time-invariant. The peak potential in AC voltammetry is directly related to the formal redox potential of the substance as

$$E_p = E^{o'} + \frac{RT}{nF} \ln \frac{D_R^{1/2}}{D_O^{1/2}} \qquad (1.9)$$

where E_p represents the peak potential, $E^{o'}$ the formal redox potential, D_R and D_O the diffusion coefficients of the reduced and oxidized species respectively. *R, T, n* and *F* have their usual meanings.

This technique provides more information than the dc voltammetry techniques. Many advantages accrue to this technique such as experimental ability to make high-precision measurements because the response may be indefinitely steady and therefore can be averaged over a long time and also due to the ability to treat the response theoretically by linearized current-potential characteristics.

1.3.3.2.4 Pulse Voltammetry

In order to increase speed and sensitivity, many forms of potential modulation (other than just a simple staircase ramp) have been developed. The excitation signal in pulse voltammetry consists of a pulse superimposed on the linear variation of potential. Three of these pulse techniques, shown in Fig. 1.7, are widely used.

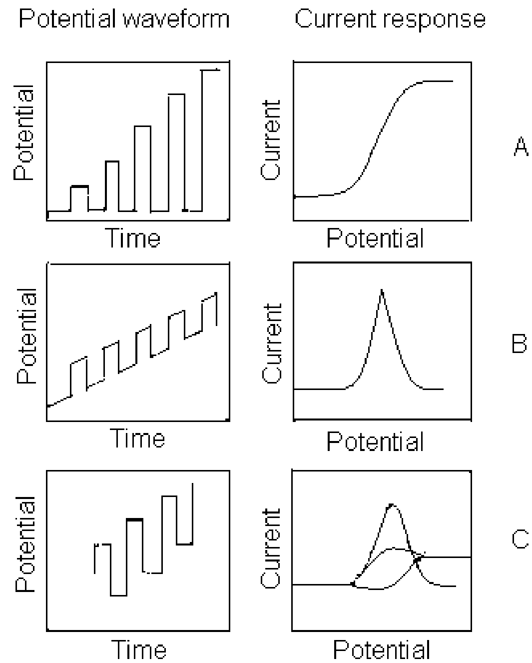

Figure 1.7: Potential waveforms and their respective current response for Normal pulse (A) Differential pulse (B) and Square-wave voltammetry (C).

Normal Pulse Voltammetry (NPV): This technique uses a series of potential pulses of increasing amplitude. The current measurement is made near the end of each pulse, which allows time for the charging current to decay.

Differential Pulse Voltammetry (DPV): This technique is comparable to normal pulse voltammetry in that the potential is also scanned with a series of pulses. However, it differs from NPV because each potential pulse is fixed, of small amplitude (10 to 100 mV), and is superimposed on a slowly changing base potential. Current is measured at two points for each pulse, the first point just before the application of the pulse and the second at the end of the pulse. The difference between current measurements at these points for each pulse is determined and plotted against the base potential.

The peak potentials in differential pulse voltammograms are directly related to the formal redox potential as

$$E_{\max} = E^{o'} + \frac{RT}{nF}\ln\left(\frac{D_R}{D_O}\right)^{1/2} - \frac{\Delta E}{2} \tag{1.10}$$

where $E_{\max}$ denotes the peak potential, D_R and D_O the diffusion coefficients of the reduced and oxidized forms respectively, and ΔE the pulse amplitude. $E^{o'}$, R, T, n and F have their usual meanings.

The shape of the response function and the height of the peak can be treated quantitatively in a straightforward manner. Sensitivities better than those of NPV can be obtained using this technique.

Square-Wave Voltammetry (SWV): The excitation signal in SWV consists of a symmetrical square-wave pulse superimposed on a staircase waveform, where the forward pulse of the square wave coincides with the staircase step. The net current is obtained by taking the difference between the forward and reverse currents and is centered on the redox potential. The peak height is directly proportional to the concentration of the electro-active species and direct detection limits as low as 10^{-8} M are possible. Square-wave voltammetry has several advantages. Among these are its excellent sensitivity and the rejection of background currents. Another is the speed. This speed, coupled with computer control and signal averaging, allows for experiments to be performed repetitively and increases the signal to-noise ratio. Applications of square-wave voltammetry include the study of electrode kinetics with regard to preceding, following, or catalytic homogeneous chemical reactions, determination of some species at trace levels, and its use with electrochemical detection in high pressure liquid chromatography (HPLC).

1.4 FLOW INJECTION ANALYSIS

Ruzicka and Hansen defined Flow Injection Analysis (FIA) in 1975.[20] FIA is a simple and versatile analytical technology employed for automated wet chemical analysis, based on the physical and chemical manipulation of a dispersed sample zone formed from the injection of the sample into a flowing carrier stream and detection downstream.

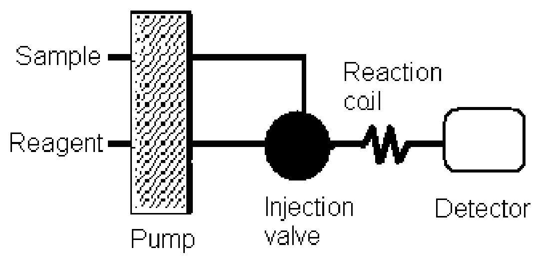

Figure 1.8: Basic components of FIA consisting of a pump, an injection valve, tubing manifold and a downstream detector.

A typical FIA manifold is comprised of a pump, injection valve, detector, and tubing manifold as shown in Fig. 1.8. The pump is used to propel one or more streams through the detector via narrow bore tubing. These streams may be reagents, solvents, or some other medium such as a buffer. The injection valve is used to periodically introduce a small volume of sample into the carrier stream. As this sample is carried to the detector, the fluid dynamics of flow through narrow-bore tubing mixes sample and reagent, leading to chemical reaction to form a detectable species. This species is sensed by the detector as a transient peak. The height and area of the peak are proportional to concentration, and are used to quantify the concentration of the compound being determined by comparison to samples of known concentration (calibration curve).

A wide range of different sample processing steps have been integrated into FIA methodologies.[21] These include dilution, trace enrichment, solvent extraction, matrix modification, gas permeation, and reactions with immobilized reagents (Fig. 1.9). The purpose of this step is to transform the analyte into a species that can be measured by the detector and manipulate its concentration into a range that is compatible with the detector, using one or more of the indicated processes.

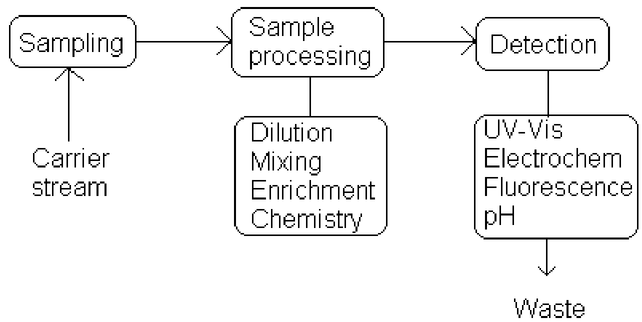

Figure 1.9: Schematic representation of FIA. The process can be grouped into three stages: Sampling, sample processing and detection.

A large variety of detectors can be used in FIA. Detection is most frequently photometric. Electrochemical techniques such as amperometry, and potentiometry, have gained new life by coupling them to flow-based sample handling techniques such as FIA and SIA (Sequential Injection Analysis).

Sequential Injection Analysis (SIA) is a second-generation approach to FIA compatible assays. SIA typically consumes less than one-tenth the reagent and produces far less waste – an important feature when dealing with expensive chemicals, hazardous reagents, or online/remote site applications. One disadvantage of SIA is that it tends to run slower than FIA.

Most recently, FIA is used in biology for study of live cells by fluorescence microscopy and flow cytometry. Other areas of application include monitoring of chemical processes in real time, biotechnology, and immunoassays involving antibody/antigen reactions.

1.5 ELECTROCHEMICAL BIOSENSORS

An electrochemical biosensor has been defined as a "self-contained integrated device, which is capable of providing specific quantitative or semi-quantitative information using a biological recognition element retained in direct spatial contact with an electrochemical transduction element".[22] Electrochemical transducers prevail over other methods of transduction. Electrochemical biosensors based on the electron transfer between the enzyme and the electrode are especially promising. Various direct and indirect methods have been used for this purpose. Since the first proposal of the concept of an enzyme-based biosensor by Clark, Jr.,[23] significant progress in this field has been achieved.

1.5.1 Direct electron transfer

The redox-active component of most redox-enzymes is encapsulated deep inside the enzyme structure. This spacial isolation from the bulk environment also helps in the chemical and electrochemical isolation of the redox-center, allowing it to be out of equilibrium with the protein's surroundings. The imbalances that result facilitate the selective and directed chemical and electrochemical processes that sustain life. In an effort to gain understanding of these processes, the distance dependence of electron-transfer rates in proteins has been extensively studied both experimentally[24] and theoretically.[25] According to the Marcus electron-transfer theory, the electron-transfer rate constant between a donor-acceptor pair is given by,

$$k_{et} \propto \exp\left[-\beta\left(d-d_o\right)\right]\exp\left[\frac{-\left(\Delta G^\circ+\lambda\right)^2}{4RT\lambda}\right] \qquad (1.11)$$

where ΔG° and λ correspond to the free energy and reorganization energy accompanying electron-transfer, and d_o and d are the Van der Waals distance and actual distance separating the donor and acceptor centers. If one views the electrode and the enzyme redox-center as a donor-acceptor pair, it becomes clear that the thick protein layer surrounding the active-center provides an effective kinetic barrier to electron-transfer.[26]

The ability of the enzymes to directly contact the electrode is therefore attributed to the peripheral location of the redox-center. However, certain enzymes or redox proteins can exhibit electrical communication with electrode under certain conditions.[27]

1.5.2 Mediated electron transfer

The electrical contact of redox-enzymes that defy direct electrical communication with the electrodes can be established by using synthetic or biologically active charge-carriers as intermediates between the redox-center and the electrode. These artificial electron donor or acceptor molecules (in case of reductive or oxidative enzymes, respectively), usually referred to as electron-transfer mediators, can be accepted by many redox-enzymes in place of their natural oxidants or reductants.[28] They have a wide range of structures, and hence properties, including a range of redox potentials. In the process of shuttling charge between the redox-center and the electrode, the mediator is cycled between its oxidized and reduced states. The redox potential of a suitable mediator should therefore provide an appropriate potential gradient for electron-transfer between an enzyme active site and an electrode. The redox potential of the mediator, E^0_M, should be more positive or more negative than the redox potential of the enzyme active site, E^0_E, in the case of oxidative ($E^0_M > E^0_E$) and reductive ($E^0_M < E^0_E$) bioelectrocatalysis, respectively.

An efficient electron mediator should possess the following characteristics:

(i) It should be stable in both the reduced and the oxidized forms and any side reactions with the enzyme or the environment should be absent.

(ii) To be effective in its role, the mediator must often compete with the enzyme's natural substrate (e.g. molecular oxygen in case of oxidases), effectively and efficiently diverting the flow of electrons to and from the electrode.

(iii) It should provide rapid reaction with the redox-enzyme, effectively oxidizing or reducing the enzyme active center.

(iv) It should also exhibit a reversible electrochemistry (a large rate constant for the interfacial electron-transfer at the electrode surface).

The total efficiency of the electron transport provided by mediators depends not only on the mediator properties, but also on the whole system architecture. A mediator that cannot compete with the natural molecular oxygen electron acceptor when it is functioning via a diffusional route could be very efficient when it is included into an organized supra-molecular assembly and operates in a non-diffusional mode. The development of these efficient electrical contacting methodologies has resulted in the construction of numerous amperometric biosensors and bioelectrocatalytic systems including bioreactors and biofuel cells.[29-31]

1.5.2.1 Diffusional mediators

Mediated electron-transfer (MET) can be affected by a diffusional mechanism where the electron relay is either oxidized or reduced at the electrode surface. The mediators diffusionally shuttle electrons between the electrode and enzymes as shown in Fig. 1.10 where the enzyme is reduced in presence of the substrate and is oxidized back by the reduction of the mediators present in the medium. The reduced mediators (M) are electrochemical oxidized (M^+) near the electrode surface. The mediators can exist in several configurations: soluble,[28] immobilized as monolayers (or multilayers),[32,33] or incorporated into porous matrices.[34,35] In all these cases the medium needs to provide a free diffusion pathway between the conductive support (providing electrochemical regeneration of the mediator) and the enzyme molecules (working as biocatalysts).

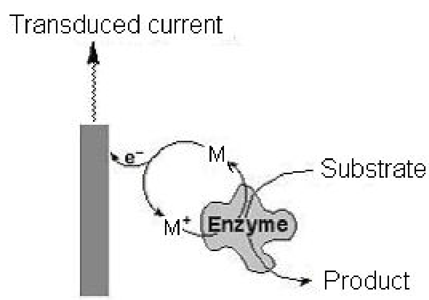

Figure 1.10: Electron transfer mechanism of an oxidative redox enzyme using diffusional mediators shuttling between the enzyme reaction center and the electrode. M represents the mediator.

Diffusional penetration of the oxidized or reduced relay into the protein yields a sufficiently short electron-transfer distance for the electrical activation of the biocatalyst. Penetration of the mediator close to the enzyme active center inside the protein matrix is controlled by the hydrophobic/hydrophilic properties of the mediator and the enzyme, the size and shape of the mediator and the electrostatic charge interactions between the mediator and the enzyme.

1.5.2.2 Mediator functionalized electrodes

The electrochemical contacting of solution-state enzymes with surface-immobilized redox-mediators is of interest for studying of the interfacial association affinity interactions between enzymes and mediators. The electrochemical kinetics of electrodes functionalized with layers of various mediators (e.g. viologens,[36] C_{60}-derivative,[37] microperoxidase-11[38]) has been studied upon their interaction with diffusionally free enzymes.

As these systems operate in the presence of soluble enzymes, they have little potential for practical purposes. However, the study of these systems has revealed temporary affinity association of the enzyme molecules with the mediator functionalized electrode surfaces (e.g. MP-11). This in turn has allowed the development of integrated biocatalytic systems composed of mediators and enzymes by the lateral cross-linking of the enzyme-mediator affinity complex generated at the electrode support.

1.5.2.3 Mediator modified enzymes

The chemical modification of redox enzymes with electron relay groups can enable non-diffusional mediated electron-transfer, often referred to as the electrical 'wiring' of the proteins[39-41] as shown in Fig. 1.11.

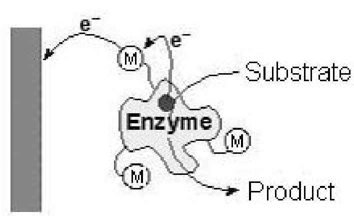

Figure 1.11: Electron transfer mechanism in mediator modified enzymes. The enzyme is electrically contacted with an electrode surface *via* redox-mediator groups covalently tethered to the protein backbone. M denotes the mediator.

The covalent attachment of electron-relay units at the protein periphery as well as inner sites, yields short inter-relay electron-transfer distances. The simplest systems of this kind involve electron relay-functionalized enzymes diffusionally communicating with electrodes,[42] but more complex assemblies include immobilized enzymes on electrodes as integrated assemblies.[40]

While an increased loading of an electron mediator on a protein enhances the effectiveness of electrical contacting, the enzyme activity suffers due to changes brought about in its structure. Therefore optimum loading of the mediator on a protein is required. Longer spacer groups bridging the electron relay groups and the enzyme provide higher mobility, shorten the electron-transfer distance, and thus enhance the enzyme's bioelectrocatalytic activity.[41]

Cross-linkers: Various cross-linkers and coupling reagents can be used for functionalizing the enzymes with the mediators. Cross-linkers are chemical reagents used to conjugate molecules together by a covalent bound. Several atoms usually separate the two molecules, forming the 'spacer arm'. Crosslinkers have become important tools for preparation of conjugates used in a lot of immunotechnologies, and for protein studies. "Crosslinking" reagents contain two reactive groups which may be similar incase of homobifunctional crosslinkers such as thiol-reactive crosslinker bis-((N-iodoacetyl)piperazinyl)sulfone rhodamine, amine crosslinkers, glutaraldehyde, bis(imido esters), bis(succinimidyl esters), diisocyanates, diacid chlorides, polyethyleneglycoldiglycidylether etc. The reactive groups can be different incase of heterobifunctional crosslinkers such as succinimidyl acetylthioacetate (SATA), 4-azido-2,3,5,6-tetrafluorobenzoic acid, 4-benzoylbenzoic acid succinimidyl ester (ATFB, SE), succinimidyl ester, etc.

An additional variation is the "zero-length" coupling reagent — a reagent that forms a chemical bond between two groups without itself being incorporated into the product. Carbodiimides, which are used to couple carboxylic acids to amines, is an example of a zero-length coupling reagent.[43]

1.6 REDOX DYES OR INDICATORS

Dyes have a wide range of application in biology. Many natural dyes have been known for long times which are obtained from animal and plant sources.[44] Today, practically all dyes are synthetic and are prepared from aromatic compounds. Many of these dyes show fluorescence characteristics. Many of these dyes have been synthesized specifically for monitoring biological redox systems.

Fluorescence: Fluorescence is the phenomenon in which absorption of light of a given wavelength by a fluorescent molecule is followed by the emission of light at longer wavelengths. Fluorescence is found in compounds containing aromatic functional groups and those with highly conjugated double bonds. The technique of spectrofluorimetry is most accurate at low concentrations, unlike absorption spectrophotometry due to increased sensitivity, which is adjustable over a large range by amplification of the detector signal. Susceptibility to pH, temperature, solvent polarity and quenching are the major disadvantages of fluorescence.

Redox dyes are dyes, which show different characteristics in oxidized and reduced form. They have a dual advantage as they act as candidates in both spectrophotometric and electrochemical detection. For practical purposes such oxidation – reduction indicators can be divided into two categories: those with relatively low potential –0.3 V to +0.5 V in neutral solution which are especially usefully for the study of biological systems, and those of more negative potentials that are employed in volumetric analysis.[45] Many of the substances proposed as oxidation – reduction indicators for biological purposes are also acid – base indicators, exhibiting different colors in acid and alkaline solutions. A few typical redox dyes used in biological work, together with their standard redox potentials at pH 7 are given in Table 1.2. These indicators can be successfully used as electron mediators in biosensors.

Table 1.2: Oxidation – reduction indicators used in biological work

Indicator	$E^{o'}$
2,6 - Dichlorophenol indophenol	-0.217
Toluylene blue	-0.115
Cresyl blue	-0.047
Methylene blue	-0.011
Indigo trisulphonate	0.081
Indigo disulphonate	0.125
Cresyl violet	0.173
Phenosafranine	0.252
Methyl viologen	0.445

CURRENT APPROACH

Many biological substances are not electroactive by themselves, as they are basically not designed by nature for that purpose. In many redox enzymes their redox active groups are found embedded deep inside the protein making them non-electroactive. For this reason various redox substances are used as mediators to shuttle electrons from the active site region to the electrode surface.

Various inorganic mediators such as hexacyanoferrate, hexacyanoruthenate and pentaamine pyridine ruthenium have been used as diffusional mediators with oxidases such as sarcosine oxidase and lactate oxidase.[46] But inorganic mediators are difficult to 'tune' for solubility and electrochemical properties as they cannot be modified or derivatized as easily as their organic counterparts. The majority of these problems have been overcome by the use of ferrocene derivatives as electron acceptors for soluble oxidases (e.g. GOx). A number of artificial electron acceptors including organic dyes such as phenazine methosulfate, and 2,6-dichlorophenolindophenol, have been used as diffusional mediators.[47] To enhance the electrical communication, diffusional mediators have been used to shuttle electrons between the conductive electrode support and the enzymes incorporated into the polymeric film.[48,49] Table 1.3 shows some of the diffusional mediators used for immobilized enzymes.

Table 1.3: Diffusional mediators used with immobilized enzymes

Enzyme	Mediator	Mediator redox potential /mV vs SCE	Ref
Glucose oxidase	1,1-dimethylferrocene	100	50
	phenazine methosulphate	-161	51
Peroxidase	$[Fe(CN)_6]^{4-}$	180	52
Cholesterol oxidase	Ferrocene carboxylic acid	275	53
NADH dehydrogenase	Ferrocenylmethanol	185	54

The chemical modification of the immobilized enzymes has been considered to develop an elegant non-diffusional route for establishing a communication link between the enzymes and the electrodes.[39,55] It is not required to have large number of mediator molecules for this purpose but instead they need to be in the right location.

The covalent attachment of electron-relay units at the protein periphery as well as inner sites, yields short inter-relay electron-transfer distances. Though this approach has been used with many enzymes[56] the vast array of redox dyes as possible mediators remains untapped. Structure, shape and the redox potential of the dyes are the primary parameters that must be evaluated for optimum performance.

In our present work we have studied the use of redox dyes which have a dual advantage of spectroscopic and electrochemical detection for use as non-diffusional mediators in biosensors. The work mainly aims at studying -

(i) The spectroscopic and electrochemical properties of redox dyes such as Neutral red, Safranine O, Nile blue A, Brilliant cresyl blue And Toluidine blue.

(ii) The electrochemical and spectroscopic properties of the dyes bound to a test protein bovine serum albumin.

(iii) The electrocatalytic effect of redox dyes covalently bound to enzymes horseradish peroxidase and glucose oxidase.

(iv) The enhancement in the enzymes bioelectrocatalytic activity on using longer spacer groups bridging the redox dyes and the enzyme.

SPECTROSCOPIC AND ELECTROCHEMICAL STUDIES ON REDOX DYES

2.1 INTRODUCTION

Many biological substances are not electroactive by themselves, as they are basically not designed by nature for that purpose. Proteins, especially enzymes that are widely used for biosensor application are not electroactive in general. Some enzymes like alchohol dehydrogenase, nitrate reductase, glucose oxidase, nitrite reductase, ubiquinone oxidoreductase, dopamine-β-monooxygenase contain redox active groups such as NAD, NADP, FAD, cytochrome, quinone, and ascorbate respectively. These redox groups are often shielded from the surface due to the presence of a protein shell round them. Therefore the electroactivity of the enzymes is dependent on the surface location of these redox groups. In many enzymes these redox groups are found embedded deep inside the protein making them non-electroactive.

For this reason various redox substances are used as mediators to shuttle electrons from the active site region to the electrode surface. Redox dyes which have a dual advantage of spectroscopic and electrochemical detection can be and often are used as electron – transfer mediators. These dyes have a wide range of structures, and hence properties, including a range of redox potentials. The binding of the dyes to the protein makes the protein electroactive by proxy and help in monitoring the electrochemical and spectroscopic changes associated with various processes related to the proteins like enzyme-substrate binding, hormone-acceptor binding, antigen-antibody binding, etc. The binding of the dyes to the proteins enables non-diffusional mediated electron-transfer from the active site of the enzyme to the electrode surface.

We have studied the use of dyes such as Neutral red, Safranine O, Nile blue A, Brilliant cresyl blue and Toluidine blue as electron mediators. These dyes are aromatic compounds showing redox behavior at considerably low potentials compared to diphenylamines whose potentials are greater than 720 mV. The presence of a reactive amino group in all of the dyes selected for our study makes them suitable for covalently coupling them to proteins. The wide range of application of these dyes in biological work and their easy availability is one of the major reasons for selecting these dyes in the present study.

2.1.1 Dyes used in the present study

<u>*Phenazines*</u>: These are basically three six membered ring structures with two nitrogens in the central ring in the para position as shown in Fig. 2.1. Neutral red and Safranine O belong to this class.

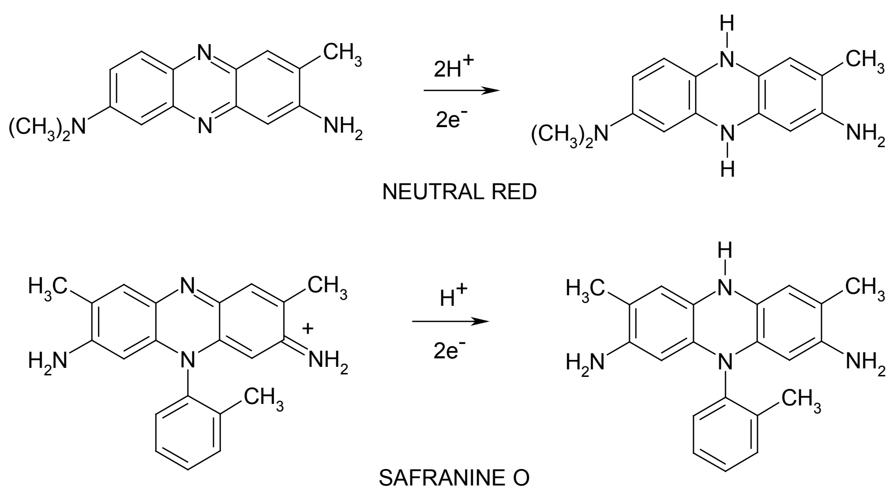

Figure 2.1: Structures of the two phenazine dyes used in our study: Neutral red and Safranine O. The oxidized form of the dyes is shown on the left and the reduced form on the right. From the redox reaction it is apparent that the redox potentials are pH dependent.

<u>*Phenoxazines*</u>: These resemble the basic structure of phenazines except that one of the nitrogen in phenazines is substituted by an oxygen atom as shown

in Fig. 2.2. Nile blue A and Brilliant cresyl blue belong to the class of phenoxazines.

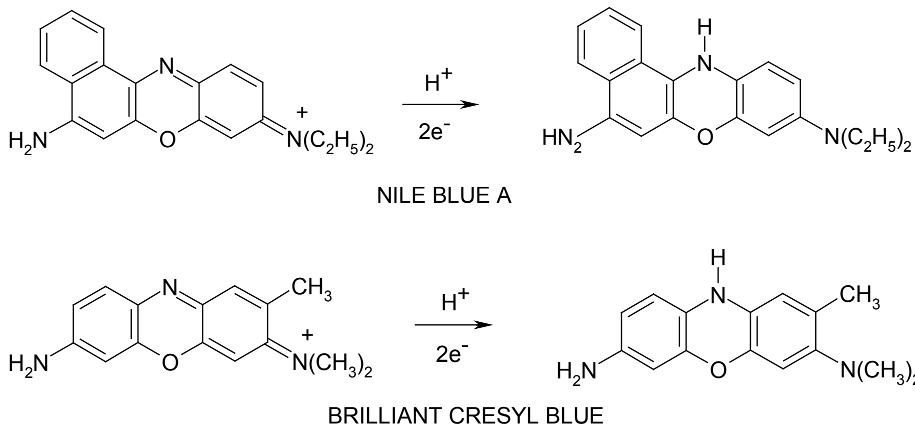

Figure 2.2: Structures of the two phenoxazine dyes used in our study: Nile blue A and Brilliant cresyl blue. The oxidized forms of the dyes are shown on the left and the reduced forms on the right. The redox process shows that the redox potentials are pH dependent.

Phenothiazines: These are also basically three six membered ring structures resembling phenazines wherein one of the nitrogen atoms in the central ring is replaced by a sulphur atom. Toluidine blue belongs to the class of phenothiazines whose structure is shown in Fig. 2.3.

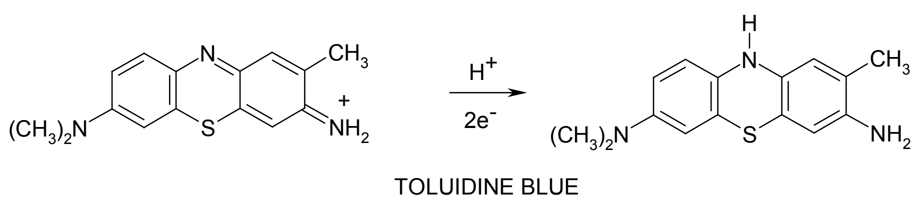

Figure 2.3: Structure of the phenothiazine class of dyes used in the present study: Toluidine blue. The oxidized form is shown on the left and the reduced form on the right. It is apparent from the redox process that the redox potential is pH dependent.

2.1.2 *Redox properties of the dyes*

The net redox processes of these dyes in aqueous systems are two electron and proton dependent reactions, the number of protons participating in the reaction being determined by the pK_a values of the reduced and oxidized forms. The redox potentials of the dyes used in our study are given in Table 2.1.[57]

Table 2.1: Redox potentials of the dyes used in the present study at pH 7

Dye	Redox potential vs SHE (mV)
Neutral red	-325
Safranine O	-289
Nile blue A	-119
Brilliant cresyl blue	47
Toluidine blue	34

2.1.3 *Spectroscopic properties of the dyes*

Neutral red changes its color from red to yellow over a pH range of 6.8 to 8.[58] Safranine O is red in color at all pH. Nile blue A is blue in color in acidic and neutral pH but red at higher pH (above 8).[57] Brilliant cresyl blue and Toluidine blue are blue at all pH.

All these dyes are leucodyes and therefore on reduction, these dyes become colorless. The reduced forms are easily oxidized back in presence of oxygen. Neutral red and Safranine O behave partly as a reversible system but undergoes a secondary irreversible change under certain conditions (vide infra).

Dyes used in our study also show fluorescence. Their fluorescence is auto-quenched at higher concentrations. The colourless reduced species of

Neutral red and Safranine O if kept under air free conditions rapidly develop fluorescence. The formation of the fluorescent material causes potentials to be erratic and to drift rapidly.[57] The fluorescent substance itself is not rapidly oxidized by air. The absorption λ_{max} and emission λ_{max} of the dyes used in this study are shown in Table 2.2.

Table 2.2: Spectroscopic properties of the dyes at neutral pH: Absorption (Abs) and emission (Em) wavelengths.

Dye	Abs λ_{max} (nm)	Em λ_{max} (nm)
Neutral red	530	600
Safranine O	520	580
Nile blue A	625	670
Brilliant cresyl blue	630	640
Toluidine blue	600	670

2.1.4 Applications of the dyes in biology

Neutral red: It has been widely used in many staining methods, but its common use is as a simple red nuclear counter stain. It has also been incorporated into bacteriological growth media as a pH indicator since it changes its color from red to yellow over the pH range 6.8 - 8.0.[59]

Safranine O: It is most commonly used for counterstaining nuclei red and cartilage yellow. It is widely used as a counter-stain in gram staining.

Nile blue A: It forms a red staining lysochrome, named Nile red, when it is boiled with dilute sulphuric acid. An aqueous mixture of Nile red and Nile blue A will preferentially stain lipids from the solution, colouring them red and in contrast stains the nuclei and background blue.

Brilliant cresyl blue: It is widely used in staining of reticulocytes.[60] It is recommended as an indicator, being blue in most solutions, at all pH and colourless when reduced.[61]

Toluidine blue: It is a blue nuclear counter-stain. It is also used for staining mast cell granules.

The fluorescent property of Neutral red and Safranine O is used for staining chromatin, where the dye intercalates with the chromatin.[62,63] The fluorescent property of Nile blue A is used to detect malignant tissues.[64] Toluidine blue is used as a counter-stain for lipophylic fluorescence tracers.[65]

In the present study, electrochemical properties of the redox dyes on a glassy carbon electrode are studied. The spectroscopic and electrochemical properties of the redox dyes on covalent binding to a test protein BSA using a coupling reagent 1-ethyl-3-(3-dimethylaminopropyl)carbodiimide (EDC) is studied.

2.2 MATERIALS AND METHODS

2.2.1 Materials

Neutral red is obtained from Acros, Safranine O and Toluidine blue from Aldrich Chemie, Nile blue A from Kodak, Brilliant cresyl blue from Fluka. 1–ethyl–3–(3–dimethyl aminopropyl) carbodiimide hydrochloride (EDC) is procured from Sigma, Sephadex G25 from Amersham Biosciences and Sephadex G50 from Pharmacia. All other reagents are locally obtained.

2.2.2 Instrumentation

Shimadzu UV-160A UV-Visible recording spectrophotometer and Hitachi F-3010 spectrofluorophotometer are used for spectroscopic studies.

Electrochemical studies are carried out on a CH Instruments Electrochemical Workstation (model 660A). A 3-electrode setup with glassy carbon as the working electrode, Ag/ AgCl as the reference electrode and a platinum coil as the counter electrode is used for the electrochemical studies.

2.2.3 Methodology

2.2.3.1 Immobilization to electrode surface

The working electrode used for our studies consists of a 3 mm diameter glassy carbon rod fixed in an insulating material. The electrode surface is polished with a polishing cloth or using alumina powder and rinsed thoroughly in distilled water and sonicated. The electro-active substance is immobilized onto the electrode surface by adsorption. 5 μl of 1mM dye solution or 5 μl of ~1mg/ml coupled sample is placed on the electrode surface and allowed to dry slowly at room temperature. The unadsorbed sample is removed by rinsing the electrode in distilled water before carry out the electrochemical experiments.

2.2.3.2 Reduction of the dyes

For some experiments the dyes are initially reduced using sodium dithionite. It is expected that the reduced dyes can show better coupling efficiency. Drops of sodium dithionite solution prepared freshly by dissolving sodium dithionite in water are added to the dyes dissolved in 0.1 M phosphate buffer of pH 7, till the dye solution turns colorless.

2.2.3.3 Covalent modification of BSA with redox dyes

200 μl of 2 mM of EDC prepared freshly in distilled water is added to a mixture containing 200 μl of 0.15 mM BSA dissolved in the reaction buffer (0.1M phosphate buffer of pH 7 when the reduced dyes are used and 0.1 M

bicarbonate buffer of pH 9 when the native dye is used) and 200 μl of 2 mM of the dye solution, and incubated overnight at room temperature. Carbodiimides react with carboxyl groups to form an intermediate that can stabilize with reaction with amines forming an amide bond.[66,67] During this reaction EDC activates the carboxyl groups present in the acidic amino acid residues of BSA. The activated carboxyl groups react with the amino group present in the side chain of the dyes to form an amide bond as shown in Fig. 2.4.

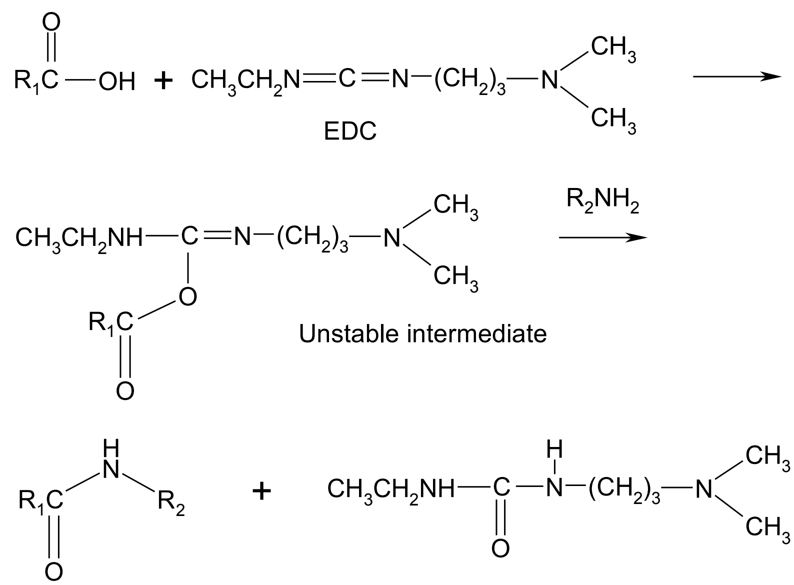

Figure 2.4: Reaction mechanism of carbodiimide as coupling agent between a carboxyl group and an amino group. R_1COOH denotes BSA and R_2NH_2 the dye.

2.2.3.4 Separation of the coupled sample from the reaction mixture

1 gm of Sephadex G25 or Sephadex G50 beads are allowed to swell in the reaction buffer overnight before packing it into a 15 ml column. The reaction mixture of 600 μl is loaded on the column equilibrated with the reaction buffer. Initial 3 ml (corresponding void volume) of the eluate is

discarded. 1ml fractions of the eluate are collected and their absorbance at the λ_{max} of the dye and λ_{max} of BSA i.e., 280 nm, and the fluorescence emitted when excited at the absorbance λ_{max} of the dye, are monitored.

2.2.3.5 Electrochemical studies

0.1 M KCl with 0.1 M phosphate buffer of appropriate pH or 0.1 M carbonate buffer of pH 9 in 1:1 ratio is used as the electrolyte. 5 ml cell volume is used for the experiments. The effect of pH and adsorption of the dye to the electrode surface is monitored using cyclic voltammetry (CV). Electrochemical studies on the dyes coupled to BSA are carried out using Differential pulse voltammetry (DPV) a more sensitive technique than CV. Effect of buffer on the electrochemical properties of the coupled dye is studied using AC voltammetry.

2.3 RESULTS AND DISCUSSION

2.3.1 Spectroscopic studies on the dyes

The fluorescent properties of the dyes in native state and on reduction with sodium dithionite are studied. The dye is dissolved in 0.1 M phosphate buffer of pH 7. No significant changes in their fluorescent properties like shift in the emission λ_{max} or in the intensity of fluorescence is observed on reducing the dyes except for Neutral Red. The fluorescence of Neutral red is not only enhanced but also the emission peak shifts to shorter wavelength on reduction. Fig. 2.5 shows the fluorescence spectra of 5 μM Neutral red in native condition and on reduction using sodium dithionite.

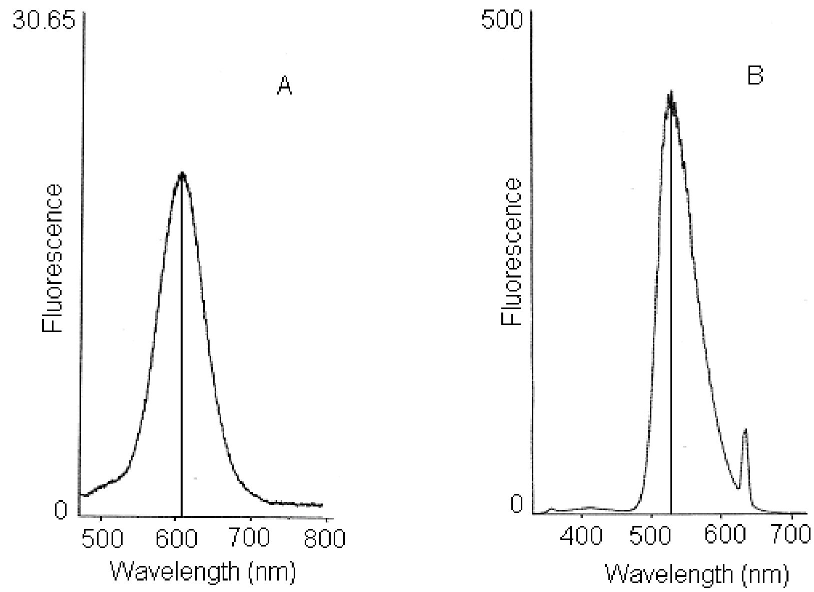

Figure 2.5: Fluorescence spectra of 5μM Neutral red in native condition (A) and on reduction (B). Excitation wavelength = Absorption λ_{max} i.e., 530 nm for native dye and 315 nm for reduced dye. The emission λ_{max} shifts from ~600 nm to ~530 nm on reduction.

It is observed that the fluorescence is enhanced ~20 times on reduction i.e., from ~20 to 400 and the emission peak shifts from 600 nm to 530 nm.

2.3.2 Electrochemical studies on the redox dyes

The electrochemical properties of the dyes in solution and on adsorbing to the glassy carbon electrode surface are studied. The variation of the formal potential $E^{o'}$, with pH, of the dyes in solution and on adsorbing to the glassy carbon surface is monitored. The variation of the $E^{o'}$ of the dyes on adsorbing to electrode when compared to that in solution is also monitored. The slope of the $E^{o'}$-pH curve indicates the number of protons involved in the redox process. A slope of –30 mV involves a single proton in the redox process, -60 mV involves two protons and –90 mV involves three protons in the redox process. As the $E^{o'}$-pH curve passes through a pH equal to pK_r (dissociation constant of the reduced form) the slope defined as $\Delta E^{o'}/\Delta pH$ will decrease by 30 mV (at 30°C) with increase in pH. Similarly, on passing through a pH equal to pK_o (dissociation constant of the oxidized form), the slope will increase by 30 mV.[68] A change in the redox potential of an electroactive substance on adsorbing to the electrode surface indicates a difference in the interaction of the oxidized and reduced forms of the substance with the electrode surface.[69] When the oxidized form of the electroactive substance interacts better with the electrode surface than the reduced form, the formal redox potential shifts to more negative value and the other way when the reduced form interacts better with the electrode surface.

Neutral red: It is observed that the overall slope of the $E^{o'}$-pH curve is close to -60 mV indicating that $2H^+$ take part in the redox process. The slope of the curve for the adsorbed dye and the dye in solution remains unchanged as shown in Fig. 2.6. This indicates that the redox characteristics of the dye at various pH are maintained even on adsorbing to the electrode surface. A significant shift of the formal redox potential ($E^{o'}$) to negative potential value on adsorption when compared to that in solution is observed. This indicates that its oxidized form interact more strongly with glassy carbon than the reduced form.

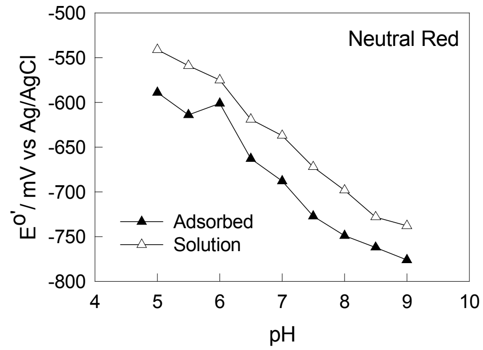

Figure 2.6: $E^{o'}$ values of Neutral red in solution and on adsorbing to glassy carbon electrode at various pH. The $E^{o'}$ values are obtained from the cyclic voltammograms. The slopes of the two curves are identical. The formal redox potential shifts to negative value on adsorbing to the electrode surface.

<u>*Safranine O*</u>: The slope of the $E^{o'}$-pH curves is close to -30 mV indicating that one proton is involved in its oxidation-reduction process. It is also observed that the slope of the curve remains unchanged on adsorption as shown in Fig. 2.7. This shows that the adsorption of the dye to the electrode does not affect its characteristics.

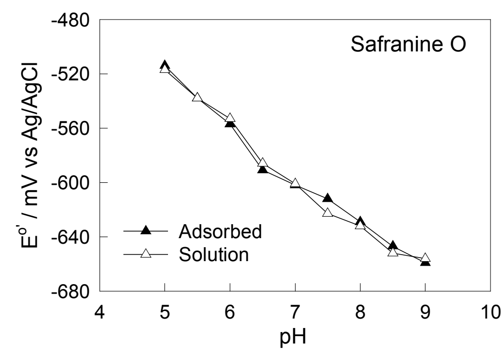

Figure 2.7: $E^{o'}$ values of Safranine O in solution and on adsorbing to glassy carbon electrode at various pH. The $E^{o'}$ values are obtained from the cyclic voltammograms. The slope of the curve is unchanged on adsorption. There is no significant change in the formal redox potential on adsorption.

<u>*Nile blue A*</u>: It is observed that the slope of the $E^{o'}$-pH curve for Nile blue A is close to –30 mV indicating the involvement of one proton in the redox process. The characteristics of the dyes on adsorbing to the electrode are not significantly effected except at low pH as shown in Fig. 2.8 where the slope

of the curve increases on adsorption indicating the chance of involvement of more number of protons in the redox reaction.

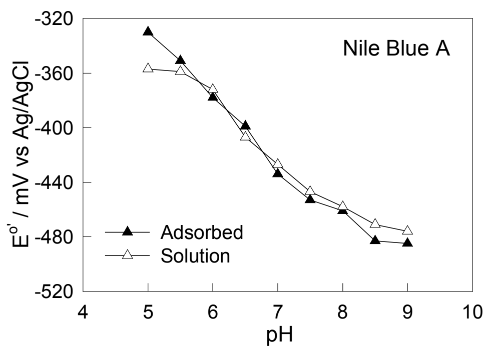

Figure 2.8: $E^{o'}$ values of Nile blue A in solution and on adsorbing to glassy carbon electrode at various pH. The $E^{o'}$ values are obtained from the cyclic voltammograms. The slope of the curve is not much affected on adsorption. There is no significant change in the formal redox potential on adsorption except at low pH.

Brilliant cresyl blue: The slope of the $E^{o'}$-pH curve indicates that two protons maybe involved in the redox process at acidic and neutral pH. The slope of the curve decreases at alkaline pH indicating the dissociation of the reduced form. The $E^{o'}$ of Brilliant cresyl blue is not much affected on adsorption at acidic and neutral pH but shifts to negative value at higher pH (Fig. 2.9). This indicates that at higher pH the oxidized form of the dye interacts better than the reduced form with glassy carbon.

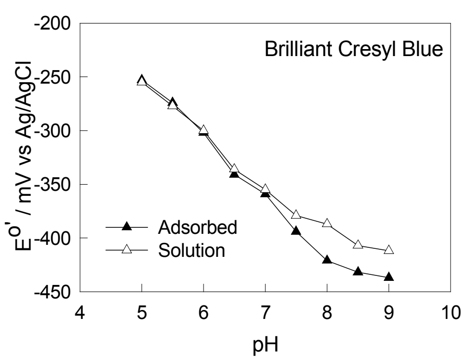

Figure 2.9: $E^{o'}$ values of Brilliant cresyl blue in solution and on adsorbing to glassy carbon electrode at various pH. The $E^{o'}$ values are obtained from the cyclic voltammograms. The formal redox potentials in acidic and neutral conditions are not much affected by adsorption but the $E^{o'}$ shifts to negative potential at higher pH on adsorbing to the glassy carbon electrode surface.

Toluidine blue: The slope of the $E^{o'}$-pH curve indicates the involvement of a single proton in solution and two protons when adsorbed on to the electrode.

This is indicated by the increase of the slope from ~-30 mV to ~-60 mV on adsorption as shown in Fig. 2.10. A significant shift of the formal redox potential ($E^{o'}$) to negative potential value on adsorption when compared to that in solution is observed, which is more significant as the pH increases indicating that its oxidized form interacts better with glassy carbon than the reduced form.

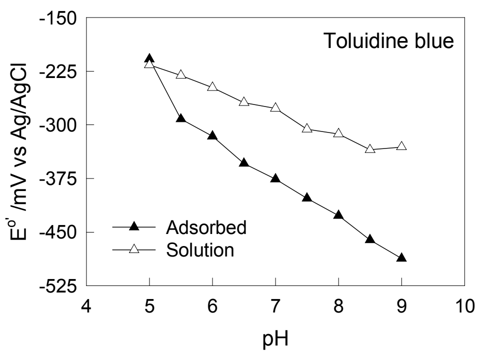

Figure 2.10: $E^{o'}$ values of Toluidine blue in solution and on adsorbing to glassy carbon electrode at various pH. The $E^{o'}$ values are obtained from the cyclic voltammograms. On adsorbing the slope of the curve increases. The formal redox potential shifts to negative value on adsorbing to the electrode surface as the pH increases.

The presence of an extra benzene ring in case of Nile blue A and Safranine O might be the reason for the stabilization of the redox potentials even after adsorbing to the electrode surface, as the extra ring is supposed to decrease the solubility of the dye in aqueous solutions. For the adsorbed dyes, a decrease in the surface coverage is observed for Neutral red, Brilliant cresyl blue and Toluidine blue on repeated cycling especially at low pH. This is due to the restricted number of aromatic rings, which makes them more soluble in aqueous solution as observed earlier for most of these dyes on a graphite electrode.[70] The decrease is more pronounced incase of Neutral red with noticeable tailing of the reduction and oxidation peaks.

2.3.3 Degree of coupling

Since the coupled sample has higher molecular weight than the free dye, it elutes faster than the free dye on a Sephadex gel column. Therefore the fraction, which elutes first from the column, that shows maximum absorbance at λ_{max} of the dye and 280 nm (λ_{max} of BSA) indicates the coupled sample. The elution profile of the reaction mixtures based on absorption indicates an initial increase in the absorbance at the λ_{max} of the dyes and at 280 nm of the fractions and then a gradual decrease and again an increase. The initial increase is due to the presence of the dye coupled protein, which elutes earlier followed by a decrease and then again an increase showing the elution of the free dye. As the dyes are aromatic in nature they also show an absorbance at 280 nm.

Fig. 2.11 shows the elution profile of the coupling reaction mixture of BSA and Safranine O based on absorbance at the λ_{max} of the dye (520 nm for native dye and 315 nm for the reduced dye) and protein (280 nm). Reaction buffer of 0.1 M bicarbonate buffer of pH 9 and native dye are used for the coupling. A simultaneous increase at 520 nm, and 280 nm is observed in fraction 3 indicating the elution of the dye coupled BSA. A decrease in the absorbance is observed in fractions eluting after fraction 3. The free dye elutes from fraction 7. The elution profiles of all the coupling reaction mixtures show a similar trend.

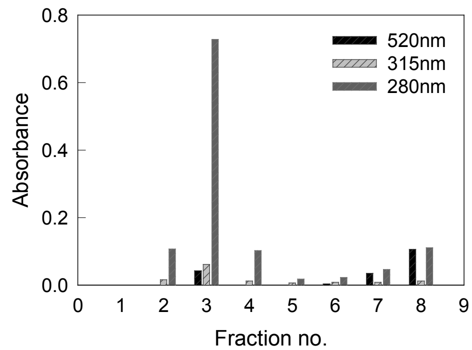

Figure 2.11: Elution profile of the coupling reaction mixture of BSA and Safranine O. The coupling reaction was carried out at pH 9. A simultaneous increase in the λ_{max} of the dye and BSA is observed in fraction 3 indicating the elution of BSA coupled with the dye. The free dye elutes from fraction 7.

The coupled sample is also confirmed from the fluorescence profile as shown in Fig 2.12. The fluorescence emitted increases in fraction 3, which contains the coupled sample and then gradually decreases. The fluorescence starts increasing after fraction 7 indicating the elution of the free dye.

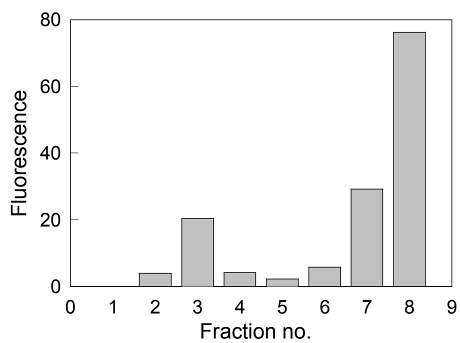

Figure 2.12: Elution profile of the coupling reaction mixture of Safranine O and BSA. Increased fluorescence is exhibited by fraction 3 indicating the elution of the coupled sample. The fluorescence gradually decreases after fraction 3 and starts increasing from fraction 7 indicating the elution of the free dye.

Fig. 2.13 shows the elution profile of the coupling reaction mixture of Safranine O and BSA at pH 7 using 0.1 M phosphate buffer. The dye is initially reduced before coupling. The coupled sample elutes in fraction 3, which is indicated by the simultaneous increase in the absorbance of the fraction at λ_{max} of the dye (520 nm for native dye and 315 nm for the reduced dye) and λ_{max} of BSA (280 nm). Though the reduced dye is used in the study, absorbance at 520 nm is also observed since part of the dye might be in the native state.

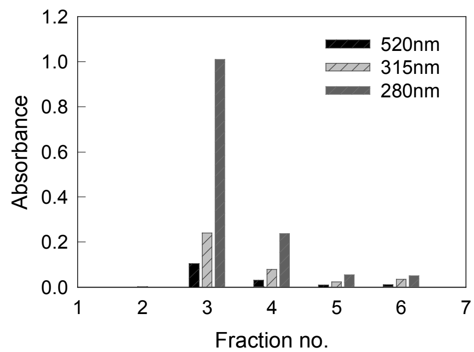

Figure 2.13: Elution profile of the coupling reaction mixture of BSA and Safranine O. The dye was initially reduced and used for coupling. The coupling reaction was carried out at pH 7. A simultaneous increase in the λ_{max} of the dye and BSA is observed in fraction 3 indicating the elution of BSA coupled with the dye. The free dye elutes much later (not shown in the figure).

The degree of coupling (DOC) i.e., number of dye molecules per protein molecule is calculated using the formula,

$$DOC = \frac{A_{max} \times MW}{[\text{protein}] \times \varepsilon_{dye}} \tag{2.1}$$

where A_{max} is the absorbance at λ_{max} of the dye, MW - molecular weight of the protein, [protein] - protein concentration in mg/ml and ε_{dye} – molar extinction coefficient of the dye. The contribution of the dye to the absorbance at 280 nm is taken into account when calculating the amount of protein present in the coupled fraction.

Fig. 2.14 shows the comparative degree of coupling when the dye is initially reduced and used and when the dye is used in the native state. It is evident that the degree of coupling is better when the dye is initially reduced and used for coupling. The values represented are only indicative and cannot be used for comparative studies between different dyes but the degree of coupling using the same dye is indicative. This number is only an approximation as we have ignored possible changes in the absorption upon coupling.

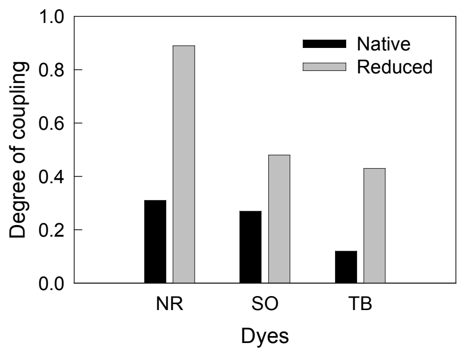

Figure 2.14: Comparative degree of coupling when the dye in native state and reduced state are used for the coupling reaction. Degree of coupling is better when the reduced dye is used.

The increase in the degree of coupling when the reduced dye is used can be attributed to the localization of the amino group in the reduced form with high reaction rate when compared to the oxidized form with delocalisation of the positive charge with low reaction rate.

2.3.4 Spectroscopic studies on dyes bound to BSA

The fluorescence emission peak of the dyes Nile blue A and Neutral red shift to shorter wavelength on binding to BSA. In case of Nile blue A the emission peak shifts from 670 nm to 655 nm on binding to BSA as shown in Fig. 2.15. This might be due to the change in the environment of the dye on binding to BSA.

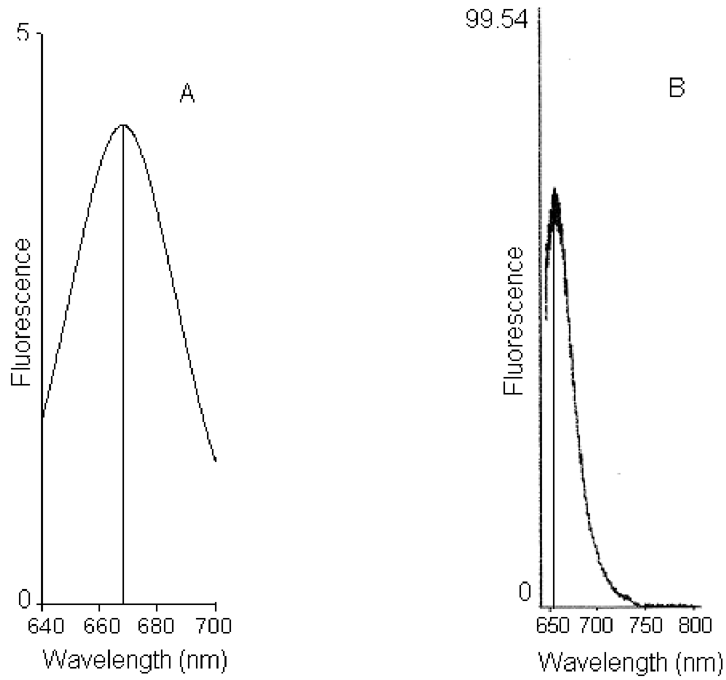

Figure 2.15: Fluorescence emission spectra of Nile blue A in free state (A) and on binding to BSA (B). The emission peak shifts from ~670 nm to ~655 nm on binding to BSA. λ_{ex} = 625 nm.

The shift is more significant in case of Neutral red as shown in Fig. 2.16 where the emission peak shifts from 600 nm to 530 nm on binding to BSA. This may also indicate that the reduced dye binds better with the protein since reduced Neutral red shows maximum emission at 530 nm as shown in Fig. 2.5B.

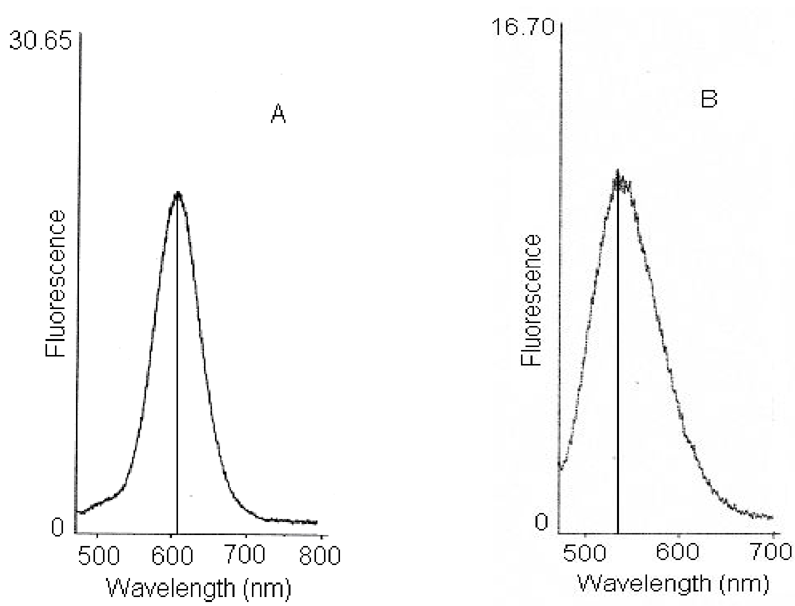

Figure 2.16: Fluorescence emission spectra of Neutral red in free state (A) and on covalently binding to BSA (B). The emission peak shifts from ~600 nm to ~530 nm on binding to BSA. λ_{ex} = 460 nm (λ_{max} of the dye at pH 9).

2.3.5 Electrochemical studies on dyes bound to BSA

Electrochemical studies on dyes bound to BSA are carried out using differential pulse voltammetry (DPV), which is more sensitive and faster than cyclic voltammetry. When the base potential is more positive or negative than the formal potential ($E^{o'}$), no faradaic current flows during the time before the pulse, and the change in potential manifested in the pulse is too small to stimulate the faradaic current. Even when the base potential is in the diffusion-limited current region, the difference in the current after and before the pulse is still small. Only in the region of $E^{o'}$ an appreciable faradaic current is observed. Only in potential regions where a small potential difference can make a sizable difference in current flow does the

DPV technique show a response. The shape of the response and the height of the peak can be treated quantitatively in a straightforward method.[71]

The peak potentials in differential pulse voltammograms are directly related to the formal redox potential as [71]

$$E_{\max} = E^{o'} + \frac{RT}{nF}\ln\left(\frac{D_R}{D_O}\right)^{1/2} - \frac{\Delta E}{2} \tag{2.2}$$

where $E_{\max}$ denotes the peak potential, D_R and D_O the diffusion coefficients of the reduced and oxidized forms respectively, and ΔE the pulse amplitude. $E^{o'}$, *R, T, n* and *F* have their usual meanings.

Using this technique the electrochemical behaviour of the dyes coupled to BSA adsorbed onto the electrode is studied. Only if the adsorbed sample is electroactive a response is observed as a peak in the differential pulse voltammograms. Assuming 100% adsorption of the sample on the electrode, the amount of the coupled sample on the electrode would be ~1nmoles/cm^2. But since glassy carbon has poor adsorption capacity and since the dye molecules coupled to BSA, which are responsible for the electroactivity of the protein, are very small when compared to the protein, the effective amount of the electroactive dye on the electrode surface is very low resulting in small peaks. A slow electron transfer between the dyes coupled to the enzyme and the electrode would also result in low response. The electrochemical investigations were performed in 0.1 M KCl and 0.1 M phosphate buffer of pH 7 in 1:1 ratio.

Figs. 2.17 and 2.18 show the differential pulse voltammograms of the various dyes covalently bound to BSA adsorbed on glassy carbon electrode.

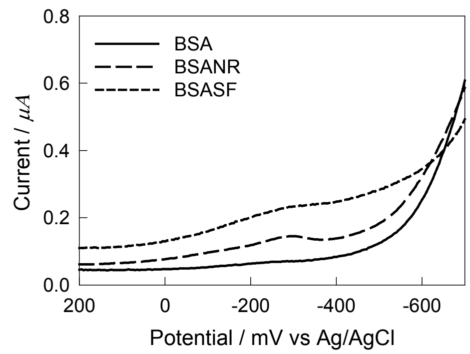

Figure 2.17: Differential pulse voltammograms of BSA and BSA coupled with Neutral red (BSANR) and Safranine O (BSASF). The electrochemical response of the coupled samples is indicated by an increase in the current (hump). Scan direction: 200 mV to -700 mV.

The coupled samples show reversible redox reactions near the electrode surface. An increase in the reduction (Fig. 2.17) and oxidation current (Fig. 2.18) indicated as a hump around –100 mV to –400 mV is observed for BSA coupled with various dyes. It is apparent from Figs. 2.17 and 2.18 that BSA coupled with phenazines i.e., Neutral red and Safranine O and BSA coupled with phenothiazine i.e., Toluidine blue show better response than BSA coupled with phenoxazines (Fig. 2.18).

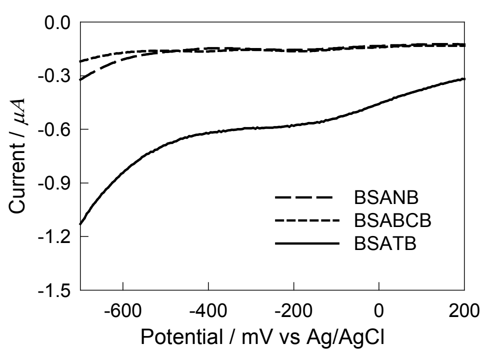

Figure 2.18: Differential pulse voltammograms of BSA and BSA coupled with Nile blue A (BSANB), Brilliant cresyl blue (BSABCB) and Toluidine blue (BSATB). The electrochemical response of the coupled samples is indicated by an increase in the current (hump). Scan direction: -700 mV to 200 mV.

These studies show that the dyes maintain their redox characteristics even after binding to the protein and thus can help in the electrochemical detection of proteins which by themselves are not sufficiently electroactive to be detected near the electrode surface and thus aid in sensing any change in the biomolecules in presence of an analyte. The $E^{o'}$ of the dyes shifts to positive potentials on binding to BSA as shown in Table 2.3. This is attributed to derivatization of the side chain amino group of the dyes.[70] The shift is more pronounced incase of dyes belonging to the class of phenazines i.e., Neutral red and Safranine O.

Table 2.3: Redox potentials of the dyes at pH 7 vs Ag/AgCl in free and bound state adsorbed on the glassy carbon electrode

Dye	Unbound / mV	Bound /mV
NR	-688	-285
SO	-602	-165
NB	-443	-190
BCB	-359	-195
TB	-376	-180

Effect of pH: Dyes that belong to the same class show similar trend in change in the reduction and oxidation peak potentials when bound to BSA, with change in pH (Fig. 2.19). The peak potentials of Toluidine blue are more or else stabilized when bound to BSA with change in pH. The slope of the curve increases drastically above pH 8 in case of Neutral red coupled to BSA indicating the involvements of more number of protons in the redox reaction.

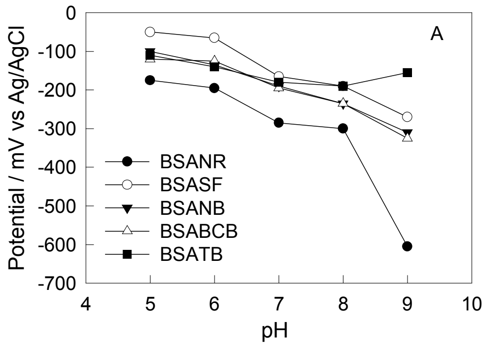

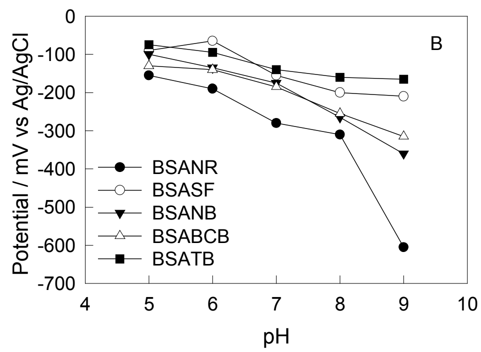

Figure 2.19: Reduction peak potentials (A) and oxidation peak potentials (B) of the dyes covalently bound to BSA adsorbed on glassy carbon electrode obtained from differential pulse voltammograms at various pH. Dyes belonging to the same class show similar trend in the change of the peak potentials with change in pH. The peak potentials of Toluidine blue are stabilized to change in pH on binding to BSA. BSANR denotes Neutral red coupled to BSA, BSASF: Safranine O coupled to BSA, BSANB: Nile blue A coupled to BSA, BSABCB: Brilliant cresyl blue coupled to BSA and BSATB: Toluidine blue coupled to BSA.

Effect of buffer constitution: The effect of buffer constitution on the redox properties of Neutral red and Nile blue A bound to BSA were investigated using phosphate buffer and carbonate buffer.

AC voltammetry: This technique involves the imposition of a sinusoidal AC voltage of about 10 mV, frequency between 100 and 100Hz, upon a linear voltage ramp of classical voltammetry.[72] Many advantages accrue to this technique such as experimental ability to make high-precision measurements because the response may be indefinitely steady and therefore can be averaged over a long time and also due to the ability to treat the response theoretically by linearized current-potential characteristics.[71] The peak potential in AC voltammetry is directly related to the formal redox potential of the substance as

$$E_p = E^{o'} + \frac{RT}{nF} \ln \frac{D_R^{1/2}}{D_O^{1/2}} \tag{2.3}$$

where E_p represents the peak potential, $E^{o'}$ the formal redox potential, D_R and D_O the diffusion coefficients of the reduced and oxidized species respectively. *R, T, n* and *F* have their usual meanings.

AC voltammetry studies on the dye coupled BSA are carried out using an electrolyte consisting of 0.1 M KCl and 0.1 M carbonate buffer in 1:1 ratio.

The ac voltammogram of Nile blue A coupled to BSA reveals a shift of the reduction peak potential of Nile blue A from –390 mV to –460 mV on covalently binding to BSA as shown in Fig. 2.20.

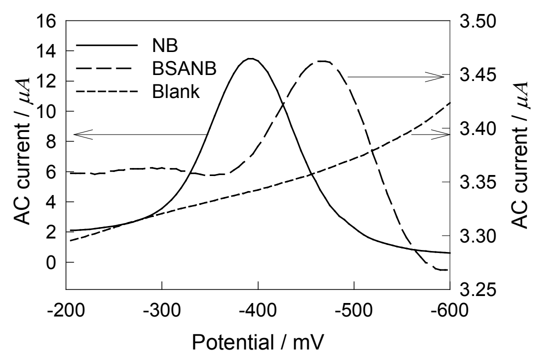

Figure 2.20: AC voltammograms of Nile blue A and Nile blue A coupled to BSA (BSANB). Scan direction: -200 mV to -600 mV. The ac voltammogram of Nile blue A shows a reduction peak at –390 mV and of Nile blue A coupled to BSA at -460 mV.

Fig. 2.21 shows that the oxidation peak potential of Nile blue A shifts from -390 mV to -430 mV on covalently binding to BSA. This shows that the redox potentials of Nile blue A coupled to BSA shift to negative values in presence of carbonate buffer unlike the case when phosphate buffer is used where a shift to positive potential is observed.

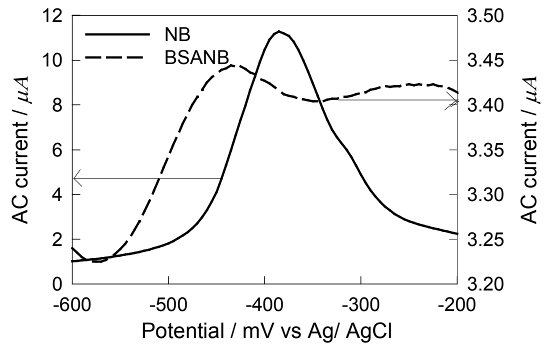

Figure 2.21: AC voltammograms of Nile blue A and Nile blue A coupled to BSA (BSANB). Scan direction: -600 mV to –200 mV. The ac voltammogram of Nile blue A shows an oxidation peak at –390 mV and of Nile blue A coupled to BSA at -430 mV.

The ac voltammogram of Neutral red coupled to BSA indicates a shift of the reduction peak potential of Neutral red on covalently binding to BSA, from –380 mV to –340 mV as shown in Fig. 2.22.

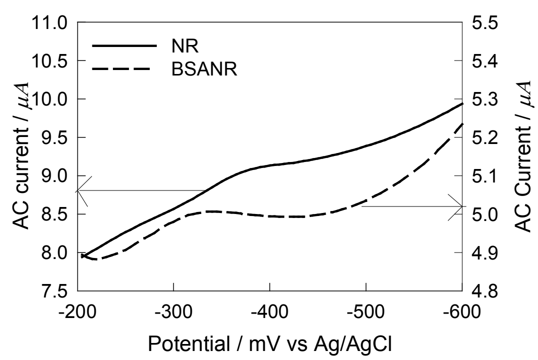

Figure 2.22: AC voltammograms of Neutral red and Neutral red coupled to BSA (BSANR). Scan direction: -200 mV to –600 mV. The ac voltammogram of Neutral red shows a reduction peak at –380 mV and of Neutral red coupled to BSA at –340 mV.

A small positive shift of the oxidation peak potential from –360 mV to -330 mV in observed for Neutral red on binding to BSA as shown in Fig. 2.23.

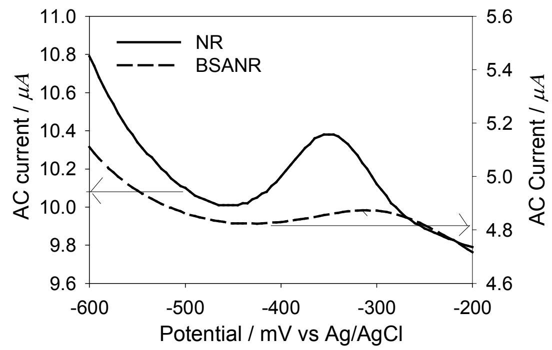

Figure 2.23: AC voltammograms of Neutral red and Neutral red coupled to BSA (BSANR). Scan direction: -600 mV to –200 mV. The ac voltammogram of Neutral red shows an oxidation peak at –360 mV and of Neutral red coupled to BSA at -330 mV.

These studies reveal that the redox potential of Neutral red shows a small positive shift on binding to BSA unlike in the case where phosphate buffer is used where a significant shift of ~400 mV to positive potential is observed.

The derivatization of the amino group of the dyes results in shifting its redox potential to positive value as discussed earlier. But the carbonate buffer effects the mediator environment increasing the electro negativity shifting the peak potentials to more negative potentials.[73] This shows that the buffer constituents also play an important role in the electrochemistry of the dyes bound to proteins (BSA).

2.4 CONCLUSIONS

The shift in the fluorescence emission peaks of the dyes Nile blue A and Neutral red on binding to BSA is attributed to the change in the environment of the dyes and also indicates that the reduced dye binds better to the protein.

The dyes maintain their redox characteristics even after binding to the protein and thus help in the electrochemical detection of proteins, which cannot be detected electrochemically.

The small shifts in the formal potentials (to positive potential) of the dyes on binding to BSA (proteins) can be used as an indication of the derivatization of the amino group of the dyes (covalent binding to the proteins).

Since the dye coupled proteins are electroactive, a change in the environment near the protein (binding of the analyte etc.) can be electrochemically detected.

ELECTROCHEMICAL STUDIES ON HRP COUPLED WITH REDOX DYES

3.1 INTRODUCTION

Determination of hydrogen peroxide (H_2O_2) is of great importance in both biological and industrial fields. It is used as a sterilizing and cleaning agent in biotechnology and food-processing industries, as an immunoenzyme marker where horseradish peroxidase (HRP) is used as a marker enzyme. It is a product of many enzyme catalyzed redox reactions.[74]

In view of the simplicity, low-cost and real-time detection properties of electrochemical techniques, these techniques have been considered for the determination of hydrogen peroxide.[75] But since the electrode kinetics of H_2O_2 is very slow at most electrode surfaces, it requires high over-potentials to drive the reaction at the electrode.[76, 77] This leads to low sensitivity and many other interferences.[78] Peroxidase is an enzyme, which is often employed to lower the activation energy for the reduction of H_2O_2 and to catalyze its electrochemical reduction at the electrode surface.[79-84] Horseradish peroxidase is a widely used peroxidase, due to its reasonable stability, commercial availability and effectiveness towards the reduction of H_2O_2.[85,86]

<u>Horseradish peroxidase (HRP)</u>

Horseradish peroxidase (EC 1.11.1.7) is a plant peroxidase obtained from a Eurasian plant *Armoracia rusticana* in the mustard family. The enzyme was first isolated by Keilin and coworkers [87] and was crystallized by Theorell.[88] Shannon *et al*., isolated seven isozymes of HRP.[89]

<u>*Structural properties of HRP*</u>: HRP is a hemin containing monomeric enzyme with a single polypeptide chain and a ferriprotoporphyrin IX prosthetic group as shown in Fig. 3.1. The polypeptide chain consists of 308 amino-acid residues with four disulphide bridges. The Ferrous atom, which

takes part in the catalytic mechanism is deeply embedded in the protein and is ~4.1 Å away from the surface of the enzyme. The enzyme shows a characteristic Soret band at 402 nm due to the heme present in it. The purity of the enzyme is expressed as RZ (reinheitszahl) units, which is the ratio of absorbance at 402 nm and 275 nm due to hemin and protein respectively.

Physical properties of HRP: Mehly has studied the physical properties of HRP.[90]

(i) *Molecular weight*: 40 KDa.

(ii) *Isoelectric point*: 7.2.

(iii) *Solubility*: 5 grams of the enzyme is soluble in 100 ml of water if traces of salts are present. In ammonium sulphate the enzyme is soluble upto 58% saturation but is insoluble above 62%.

(iv) *General stability*: The enzyme is quite stable. As a lyophilized powder, it can be stored several years, refrigerated.

(v) *pH stability*: The enzyme is stable in the pH range of 5.5 to 12 in presence of fluoride and between 4.5 to 12 in presence of other halides. Activity is terminated below pH 3.5.

(vi) *Thermal stability*: The enzyme is stable upto 63°C for 15 minutes.[91] At room temperature it is stable for several weeks.

(vii) *Oxidation-Reduction potentials*: The redox potential of the enzyme was determined by Harbury[92] and was found to be remarkably low varying from $E^{o'}$ -207 mV at pH 6.08 and $E^{o'}$ -278.7 mV at pH 7.7.

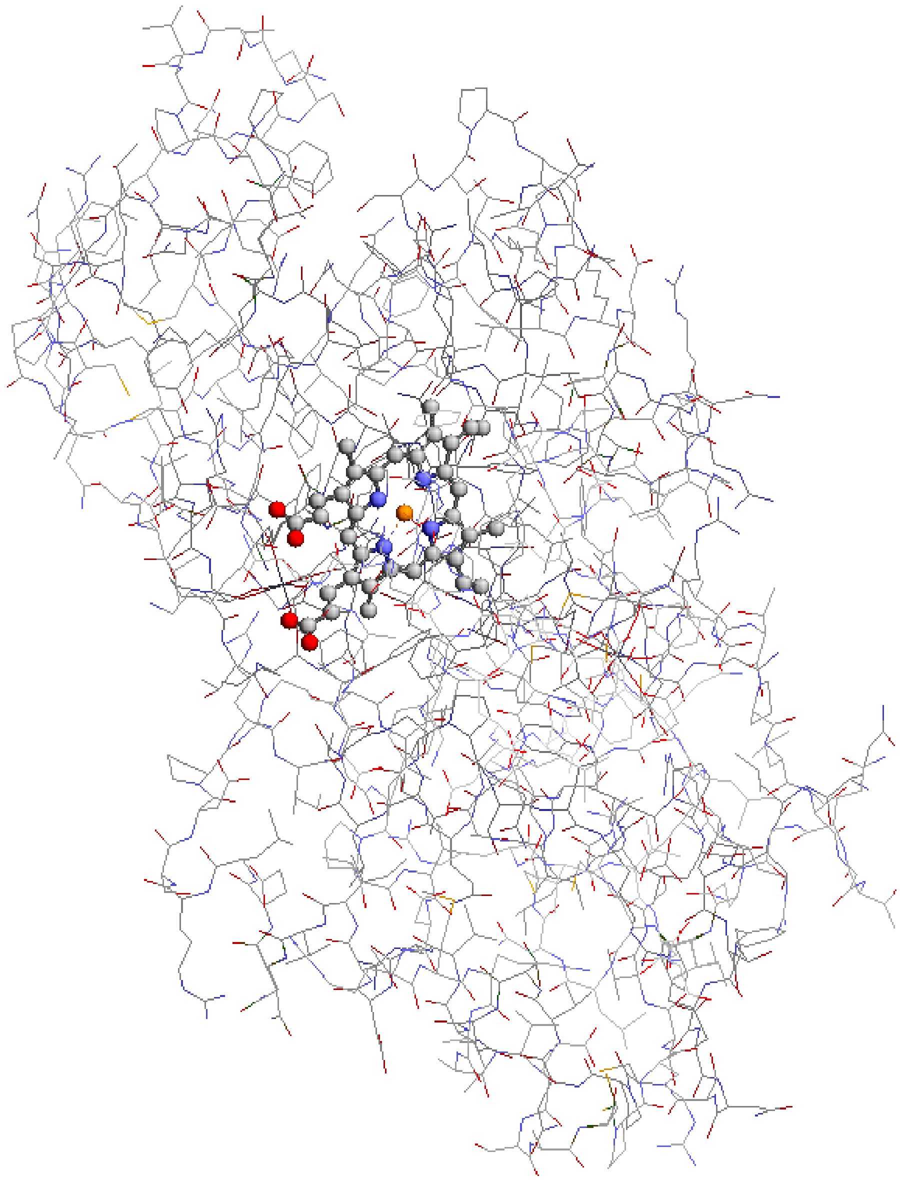

Figure 3.1: PDB structure of Horseradish peroxidase (HRP) as obtained from Swiss PDB viewer RASMOL. PDB ID: 1HCH.[93] HRP is a monomeric enzyme with 308 amino acid residues represented in stick model and the prosthetic group ferriprotoporphyrin represented in ball and stick model.

Functional properties of HRP: HRP catalyzes the oxidation of a number of electron donors such as ascorbate, ferrocyanide, cytochrome C and the leuco form of many dyes through H_2O_2 as the electron acceptor.

(i) *Reaction mechanism*: The reaction mechanism of HRP has been extensively studied.[89,90,94-96] Studies have shown that horseradish peroxidase works in 3 steps (Fig. 3.2). The first step involves the addition of H_2O_2 to the Fe III resting state of HRP, yielding Compound I. One of the H_2O_2 oxygen leaves as water, while the other is retained as a ferryl group. Compound I is two oxidation equivalents above the HRP native state. One of the equivalents is located on the ferryl group, and the other on the porphyrin. Compound I accepts one electron from a substrate molecule AH, yielding Compound II, which is one oxidation equivalent above the enzyme native state. Compound II still contains a ferryl group, but no porphyrin radical cation.[97-99] Compound II then accepts one electron from a second substrate molecule, yielding the enzyme native state.

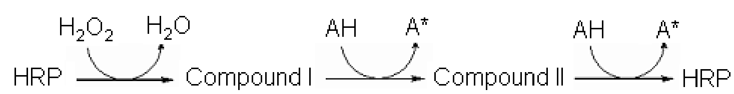

Figure 3.2: HRP general mechanism: Compound I and Compound II are the oxidized forms of HRP. AH is the reducing substrate (electron donor). Compound I is two oxidation equivalents above the native enzyme and Compound II is one oxidation equivalent above the native enzyme.

Compound III, 0, X, XI, XII, Y, I*, P670, and P630 are some other known HRP "Compounds". After Compound I and Compound II, the third important reactive intermediate of HRP is Compound III (oxyperoxidase), which is formed with excess hydrogen peroxide, or upon treatment of HRP with superoxide, or of ferro-HRP with O_2. Compound III slowly decays to Compound I and is much less reactive than the other two peroxidase Compounds.

(ii) *Substrate specificity*: The substrate specificity of HRP in forming Compound I is high. Hydrogen peroxide (H_2O_2), methyl hydrogen peroxide and ethyl hydrogen peroxide are the only compounds that could combine with HRP to form the active substrate complex Compound I.[100-102] However, the specificity of the enzyme substrate complexes for hydrogen or electron donors is quite low. Hence AH represents a number of different compounds such as 4-aminoantipyrene, cytochrome c, ferrocyanide, phenols, amino phenols, diamines, indophenols, ascorbic acid, leucodyes, and some amino acids.

(iii) *Inhibitors*: Horseradish peroxidase is reversibly inhibited by cyanide and sulfide at a concentration of 10^{-5} M.[103]

(iv) *Enzyme kinetics*: Compound II reduction is generally the rate–limiting step, with the notable exception of NO oxidation. The rate constant for H_2O_2 is 9 x 10^8 ($M^{-1}sec^{-1}$).[104] Optimum activity is observed at pH 7.

A number of electrochemical sensors for H_2O_2 using either HRP in solution or covalently immobilized or cross-linked have been reported.[105-108] However a relatively thick protein shell, hindering its direct electrical communication with the electrodes, electrically insulates the redox center or active center of HRP.[109-111] Therefore mediators have been employed to shuttle electrons between the active site of HRP and the electrodes.[112-114] The mediators can replace the natural electron donors. HRP oxidized in presence of H_2O_2 is brought back to its native state by the oxidation of the mediator, which in turn is reduced at the electrode surface.

Coupling the enzyme to the mediators enables non-diffusion mediated electron-transfer, yielding short inter-relay electron-transfer distances. Longer spacer groups bridging the electron relay groups and the enzyme provide higher mobility, shorten the electron-transfer distance, and thus enhance the enzyme's bioelectrocatalytic activity. The enzyme coupled with redox dyes can be used in optical and electrochemical biosensors.

We have coupled the enzyme HRP to redox dyes Safranine O and Neutral red to study the enhancement of the electroactivity of the enzyme near the electrode surface because of the presence of the coupled dye. Use of a spacer arm diaminohexane bridging the dye and the enzyme to further enhance the electron transfer was also studied.

3.2 MATERIALS AND METHODS

3.2.1 Materials

Horseradish peroxidase (EC: 1.11.1.7) type II (Catalog no: P 8250) and 1-ethyl–3–(3–dimethyl aminopropyl)carbodiimide hydrochloride (EDC) are procured from Sigma. 1,6–diaminohexane is obtained from Merck, glutaraldehyde from Loba Chemie, hydrogen peroxide from Qualigens, Neutral red from Acros, Safranine O from Aldrich and Sephadex G25 from Amersham Biosciences.

3.2.2 Methodology

3.2.2.1 Covalent coupling of the dyes to HRP

The dyes are initially reduced by adding drops of sodium thionite dissolved in water to 5 mM dye solution till it undergoes a change in colour (reduced). 200 µl of 5 mM EDC prepared freshly in distilled water is added to a mixture containing 200 µl of 0.25 mM HRP (10 mg/ml) in 0.1 M phosphate buffer of pH 7 and 200µl of 5 mM reduced dye solution, and incubated overnight at room temperature. The dye coupled enzyme is purified on a 15 ml G25 Sephadex column. Initial 3 ml of the eluate (corresponding void volume) is discarded. 1ml fractions of the eluate are collected and their absorbance at the λ_{max} of the dye and λ_{max} of HRP i.e., 403 nm is monitored.

3.2.2.2 Coupling of Neutral red to HRP using a spacer arm

The amino group in the dye is initially modified with glutaraldehyde and coupled to one of the amino group of diaminohexane (Fig. 3.3). The other amino group of the linker is coupled to the carboxyl groups present in the acidic amino acid residues of HRP using carbodiimide (EDC).

This is carried out in 3 steps as follows:

(i) 200 µl of 500 mM glutaraldehyde is added to 200 µl of 5 mM dye solution prepared in 0.1 M phosphate buffer of pH 7 and incubated at room temperature for 3 hours before removing the excess reagents by gel filtration on a 10 ml Sephadex G25 column.

(ii) To 500 µl of 0.25 mM of the glutaraldehyde modified dye 500 µl of 25 mM diaminohexane is added and incubated for 3 hours and purified on the Sephadex column.

(iii) Finally 100 μM of EDC is added to a mixture containing 500 μl of 25 μM HRP dissolved in 0.1 M phosphate buffer pH 7 and 500 μl of 25 μM of the dye covalently bound to diaminohexane. The reaction mixture is purified and analyzed in the similar manner to that of the dyes coupled to HRP using EDC.

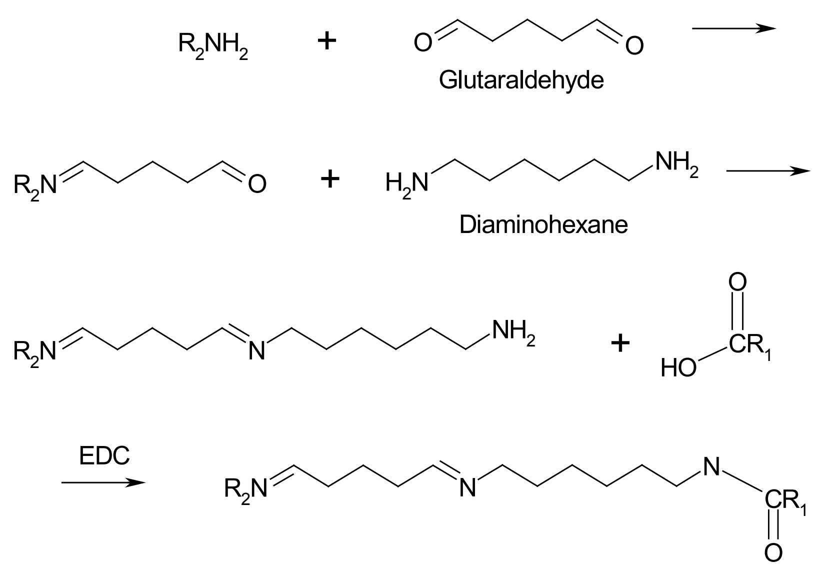

Figure 3.3: Covalent coupling of the dyes (R_2NH_2) to the carboxylic groups present in the acidic residues of HRP (R_1COOH) with a spacer arm diaminohexane using glutaraldehyde and EDC.

This process couples the dye to the enzyme with a minimum of 12-atom long spacer arm giving a greater degree of conformational freedom to the dye. Based on the concentrations used in the process, a theoretical value of 50% of coupling efficiency is expected. The possibility of glutaraldehyde polymerization in presence of oxygen might increase the length of the spacer arm.

3.2.2.3 HRP activity assay

Enzyme activity assay is carried out using a leucodye o-dianisidine, which is colorless in reduced form and colored in oxidized form. HRP is oxidized in presence of H_2O_2 and in turn oxidizes the dye, which develops an orange color whose intensity can be measured at 500 nm. The color obtained is directly proportional to the amount of oxidized HRP (enzyme activity).

2 ml of 1 mM H_2O_2 and 2 ml of 0.21 mM dye is added to 1 ml of the enzyme samples of varying concentration (enzyme units) and the absorbance at 500 nm is monitored after 5 minutes of incubation at room temperature. The standard plot is used for the activity assay of the enzyme coupled with the dyes.

3.2.2.4 Electrochemical studies on HRP coupled with redox dyes

The electrochemical experiments are carried out using a 3-electrode setup consisting of glassy carbon working electrode, Ag/AgCl reference electrode and platinum counter electrode. 0.1 M KCl and 0.1 M phosphate buffer of required pH in 1:1 ratio is used as the electrolyte.

The coupled sample is immobilized (by adsorption) on a polished glassy carbon electrode. 5 μl of ~10 μM of the sample is placed on the glassy carbon working electrode of 3 mm diameter and allowed to dry slowly at room temperature. The unadsorbed sample is removed by rinsing the electrode carefully in distilled water before carrying out the experiments. Cyclic Voltammetry (CV) and Differential Pulse Voltammetry (DPV) studies are carried out on HRP covalently bound with the redox dyes. The electrocatalytic effect of the dyes bound to HRP is studied using amperometry technique in presence of H_2O_2.

3.3 RESULTS AND DISCUSSION

3.3.1 Degree of coupling

Since the coupled sample has higher molecular weight than the free dye, it elutes earlier than the free dye. Therefore the first fraction eluted from the column, which shows maximum absorbance at λ_{max} of the dye and 403 nm (λ_{max} of HRP) indicates the coupled enzyme.

Fig. 3.4 shows the elution profile of the coupling reaction mixture of HRP and Neutral red using EDC as the coupling reagent. The coupled enzyme elutes in the 3rd and 4th fraction. The uncoupled dye elutes much latter than the coupled enzyme. The elution profiles of the other coupling reaction mixtures also show a similar trend.

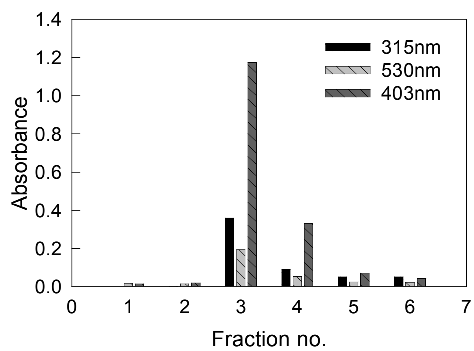

Figure 3.4: Elution profile of the coupling reaction mixture of Neutral red and HRP. A simultaneous increase in the absorbance at the λ_{max} of the dye (530 nm and 315 nm) and protein (403 nm) is observed in fraction 3 indicating the elution of the coupled sample.

The degree of coupling DOC (DOC) is calculated using the formula –

$$DOC = \frac{A_{max} \times MW}{[\text{protein}] \times \varepsilon_{dye}} \quad (3.1)$$

where A_{max} is the absorbance at λ_{max} of the dye, MW - molecular weight of the protein, [protein] - protein concentration in mg/ml and ε_{dye} – molar extinction coefficient of the dye. Approximately two dye molecules (Neutral red / Safranine O) are coupled to each protein molecule. This is only an approximation as possible changes in the absorption upon coupling have been ignored.

3.3.2 Enzyme activity assay

The amount of enzyme present in the coupled sample is estimated based on its absorbance at 403 nm (Soret band) and used for determining the activity of the enzyme using the standard calibration plot. Fig. 3.5 shows the standard calibration plot used for the enzyme activity assay.

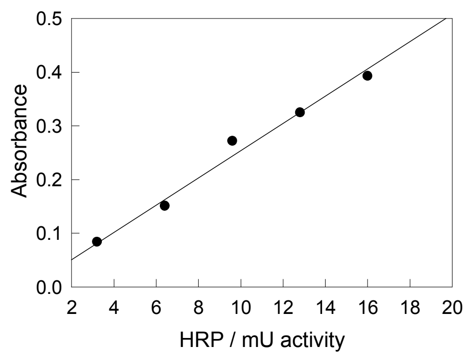

Figure 3.5: This shows the standard calibration plot for HRP activity assay using o-dianisidine. The absorbance is monitored at 500 nm. The slope of the linear graph is 0.025 A_{500} / mU activity.

We notice that the enzyme activity of the dye coupled enzyme is not much affected by the covalent binding of the dye. The specific activity of the enzyme remains practically unaltered.

3.3.3 Electrochemical studies on HRP coupled with the dyes

Fig. 3.6 shows the differential pulse voltammograms of HRP coupled with Safranine O adsorbed on glassy carbon electrode at pH 7. The initial scan shows two peaks at –90 mV and –330 mV. The second peak at –330 mV disappears in the subsequent scans. The cyclic voltammograms of HRP coupled with Safranine O also show a similar behaviour.

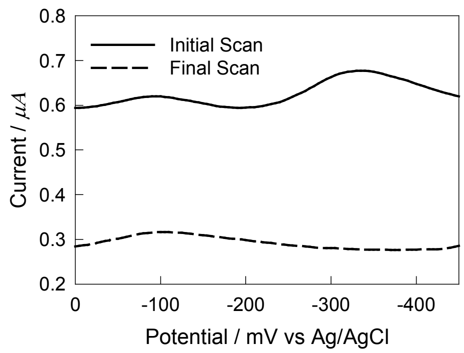

Figure 3.6: Differential pulse voltammograms of HRP coupled with Safranine O. Scan Direction: 0 mV to –450 mV. Initial scan shows two peaks at –90 mV and at –330 mV. The peak at –330 mV disappears in the subsequent scan.

The cyclic voltammograms and also the differential pulse voltammograms of HRP coupled with Neutral red adsorbed on the glassy carbon working electrode show similar electrochemical behaviour. The initial cyclic voltammograms shows two reduction peaks at –115 mV and –380 mV. The second peak at –380 mV disappears in the subsequent scans (Fig. 3.7).

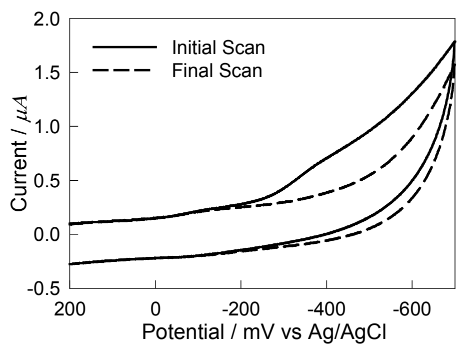

Figure 3.7: Cyclic voltammograms of HRP coupled with Neutral red. Forward scan direction: 200 mV to -650 mV. Scan rate: 50 mV. Initial scan shows two reduction peaks at -115 mV and at –380 mV. The peak at –380 mV disappears in the subsequent scan.

This behavior can be explained for a substance, which is electro-active both in dissolved and adsorbed state and where the reduced species strongly adsorbs on the electrode surface.[115] The pre-peak represents the reduction of the loosely adsorbed oxidized species to form adsorbed reduced species. This peak occurs at potentials more positive than the diffusion-controlled wave, because the free energy of adsorption of reduced species makes the reduction of oxidized species to adsorbed reduced species easier than to reduced species in solution. The second peak for reduction of the loosely adsorbed oxidized species to dissolved reduced species follows the first peak. This peak resembles that observed in absence of adsorption but is depleted during reduction of the oxidized species to adsorbed reduced species. This suggests that the reduced form of the HRP coupled with the dyes adsorbs strongly to the electrode.

In presence of the substrate H_2O_2 the strongly adsorbed reduced form of the dye coupled HRP gets oxidized. This relatively weakly bound oxidized HRP is reduced electrochemical to form the adsorbed reduced species. This reduction occurs at relatively low potential than when soluble dyes are used thus lowering the working potential of the enzyme electrode reducing the problem of interferences at higher potentials. The electrodes are found to be stable even after a week.

3.3.4 Amperometric response of the enzyme electrode to hydrogen peroxide

Fig. 3.8 shows the amperometric response of the enzyme electrodes (HRP coupled with Safranine O or Neutral red adsorbed on the electrode surface) for 2 mM H_2O_2.

The exponential decrease in the current with time fits well with an R-value of 0.999 with the three-parameter exponential decay equation,

$$y = y_o + a^{-bx} \qquad (3.2)$$

where the slope (*b* value) is related to the diffusion coefficient (D) of analyte which remains similar for all the samples analyzed. Therefore the height of the peak is directly proportional to the flux of the analyte i.e., H_2O_2 at the electrode surface given by the equation,

$$I = nAFD\left(\frac{dc}{dx}\right)_{x=0} \tag{3.3}$$

where I is current in amperes, n is the number of electrons transferred, A is the electrode area, F is the Faraday constant, D is the diffusion coefficient and dc/dx is the flux of C (analyte) at the electrode surface which is directly proportional to the concentration of the analyte.

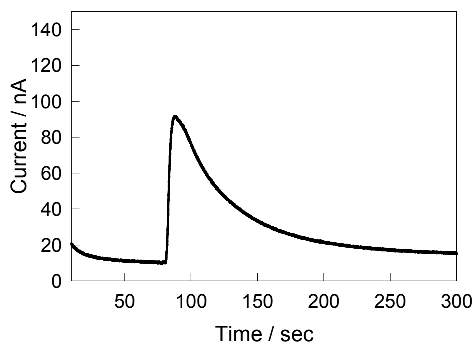

Figure 3.8: Amperometry response of HRP coupled with Safranine O adsorbed on glassy carbon electrode at a working potential of –300 mV vs Ag/ AgCl and at pH 7 in presence of 2 mM H_2O_2.

<u>*Effect of pH*</u>: Optimum enzyme activity is reported at pH 7 in case of horseradish peroxidase.[90] The effect of pH on the enzyme coupled with the dyes to H_2O_2 is investigated. The response of the enzyme electrode is optimum around the neutral pH (pH 7) for HRP coupled with Safranine O and for HRP coupled with Neutral red, which is relatively more basic than Safranine O; the response is more or less pH independent in the range of 6-8 (Fig. 3.9).

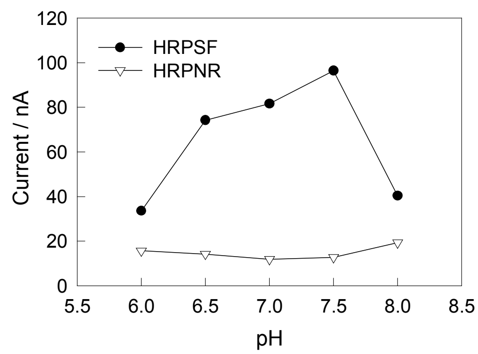

Figure 3.9: Effect of pH on the response of HRP coupled with the dyes immobilized on the electrode for 2 mM H_2O_2 at the optimum working potential. Optimum response is observed at around pH 7 for HRP coupled with Safranine O (HRPSF) and the response is pH independent in the range of pH 6-8 in case of HRP coupled with Neutral red (HRPNR).

This shows that the enzyme maintains its characteristic properties even after the dyes are covalently bound to it. Since the response is more or less pH independent in case of HRP coupled with Neutral red it is an additional useful characteristic.

Effect of working potential: Optimum response to H_2O_2 is observed at a working electrode potential of –300 mV for HRP coupled with Safranine O and at around –400 mV for HRP coupled with Neutral red as shown in Fig. 3.10.

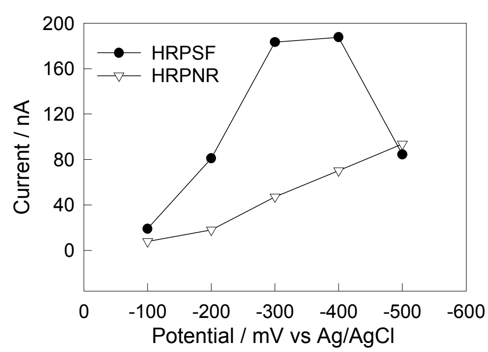

Figure 3.10: Effect of the working potential on the response of the enzyme coupled with the dyes for 2 mM H_2O_2 at pH 7. Optimum response is observed at –300 mV for HRP coupled with Safranine O (HRPSF) and around –400 mV for HRP coupled with Neutral red (HRPNR).

This shows that HRP lowers the activation energy for the reduction of H_2O_2 and also that the covalently bound redox dyes efficiently transfer the electrons from the active site of the enzyme to the electrode surface. In the absence of the dyes the insulating protein shell round the active site impairs the electron transfer between the active site and the electrode. HRP coupled with Safranine O shows optimum response at a lower working potential than HRP coupled with Neutral red.

<u>*Sensitivity of the enzyme electrodes*</u>: The enzyme electrodes show linear response to the concentration of H_2O_2 upto 500 μM concentration, as shown in Fig 3.11. Hence these biosensors can be used for quantitative studies.

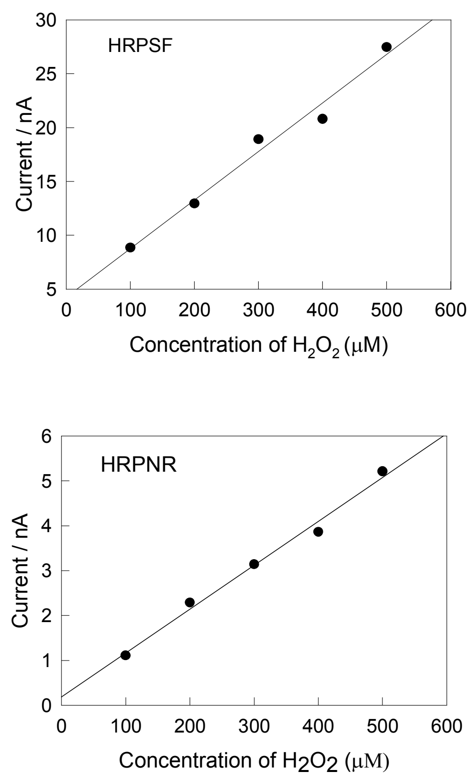

Figure 3.11: Calibration plot between H_2O_2 concentration and current response for HRP coupled with Safranine O (HRPSF) and HRP coupled with Neutral red (HRPNR). Linear response to the concentration of hydrogen peroxide is observed upto 500μM concentration.

The detection limit is 10 μM when the signal to noise ratio is 3.8 in case of HRP coupled with Safranine O and 3.5 in case of HRP coupled with Neutral red. This shows that the enzyme electrode is appreciably sensitive.

Table 3.1 shows the response of the various samples of equal concentration (0.7 nmoles/cm^2) adsorbed on the electrode surface for 2 mM H_2O_2 at optimum conditions. It is observed that the redox dyes Safranine O and Neutral red efficiently mediate the electron transfer from the active site of HRP to the electrode surface when they are covalently coupled to the enzyme. HRP coupled with Safranine O and HRP coupled with Neutral red shows ~7 times and ~2 times respectively, better response than the uncoupled HRP.

Table 3.1: Response of the various samples of equal concentration for 2 mM H_2O_2 at optimum conditions.

Sample	Response / nA
HRP	22
HRP coupled with Safranine O	154
HRP coupled with Neutral red	59
HRP coupled with Neutral red with a spacer arm	82

Effect of using a spacer arm between the enzyme and the dye: It is observed that the dyes linked to the enzyme using a spacer arm mediate the electron transfer much better than the dyes just covalently bound to the enzyme without any spacer arm. HRP coupled with Neutral red using a spacer arm diaminohexane shows nearly twice the response observed in absence of the spacer arm (Table 3.1). This reveals that a spacer arm bridging the dye and the enzyme provides higher mobility, shortens the electron-transfer distance, and thus enhance the electrocatalytic activity.

Assuming 100% adsorption on the electrode surface, the surface coverage would be ~0.7 nmoles/cm^2. But since glassy carbon does not show good adsorption capacity and since the dye molecules are very small relative to the enzyme, the effective surface coverage of the dye, which is responsible for the electrocatalytic effect, would be very small. This accounts for the low responses (small peaks). With further optimization a better response can be achieved. Since adsorption depends on various factors, a slight difference in the amount of sample adsorbed to the electrode would result in a change in the intensity of the response. As different enzyme electrodes are used for the various studies a comparative study using the different graphs cannot be made.

3.4 CONCLUSIONS

The modified enzyme is electro-active both in dissolved and adsorbed state and its reduced form strongly adsorbs to the glassy carbon electrode surface making the enzyme electrode quite stable. The peaks are small as the effective surface coverage of the electroactive dye coupled to HRP is reduced by the poor adsorption ability of the glassy carbon electrode and by the small surface coverage of the dye due to its small size in presence of the enzyme, which is relatively much larger and therefore reduces the effective surface coverage of the dye at the electrode surface.

Though the exact residue(s) on the enzyme to which the dye is coupled is not known, as the coupling reaction is not specific, covalently coupled dyes efficiently transfer the electrons between the active site of the enzyme (Ferrous atom) and the electrode surface, which otherwise is hindered by the protein shell.

HRP coupled to the dyes show better response than the native HRP for H_2O_2 as the dyes act as electron mediators between the active site of the enzyme and the electrode surface.

The characteristic properties of the enzyme such as optimum pH remains unaltered incase of HRP coupled with Safranine O. Covalent coupling of Neutral red to HRP makes the response of the enzyme nearly pH independent.

The optimum working potential for the enzyme electrode is considerably low. This overcomes the problem of various interferences at higher potentials.

The enzyme electrodes can be used for quantitative studies as linear response for the substrate concentration is observed and also the sensitivity observed is quite appreciable.

Use of a spacer arm between the enzyme and the dye further enhances the electrocatalytic activity as the spacer arm is flexible and so the dye molecules can easily take up or give electrons near the active site region as well as the distance between the active site of the enzyme and the electrode surface is reduced because of the spacer arm.

Safranine O mediates the electron transfer better than Neutral red along with lowering the required working potential and therefore with further optimizations such as using a spacer arm to bridge the enzyme and the dye, HRP coupled with Safranine O can be efficiently used for developing a successful biosensor.

ELECTROCHEMICAL STUDIES ON GOx COUPLED WITH REDOX DYES

4.1 INTRODUCTION

Glucose oxidase (GOx) is an enzyme extensively studied because of its application in determining the concentration of glucose in various clinical, biological[116] and chemical samples as well as in food processing and fermentation.[117-119] In the field of biosensors glucose oxidase based sensors are well established. Due to its ready availability, and high stability, the enzyme is an appropriate tool for glucose sensing.

Glucose oxidase (GOx)

Glucose oxidase (EC 1.1.3.4) was discovered by Maximow in 1904. It is commercially isolated from moulds belonging to the species of *Aspergillus* and *Pencillium*. Fig. 4.1 shows the overall topology of the enzyme glucose oxidase. The enzyme is a homodimer consists of two identical polypeptide chain subunits (80,000 daltons) covalently linked by disulfide bonds.[120]

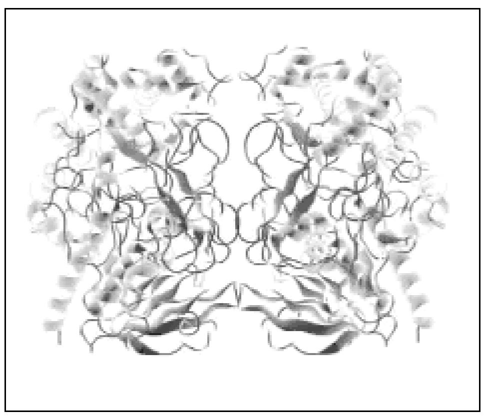

Figure 4.1: Overall topology of GOx holoenzyme (The disulphide bridges are not seen in this picture)

Each subunit consists of 583 amino acid residues and one FAD (flavin-adenine dinucleotide) molecule as shown in Figure 4.2. The enzyme is reported to be approximately 74% protein, 16% neutral sugar and 2% amino sugars.[121] The flavin ring system is located near the bottom of a deep cavity and is reported to be ~8.7Å away from the surface of the enzyme.[122,123]

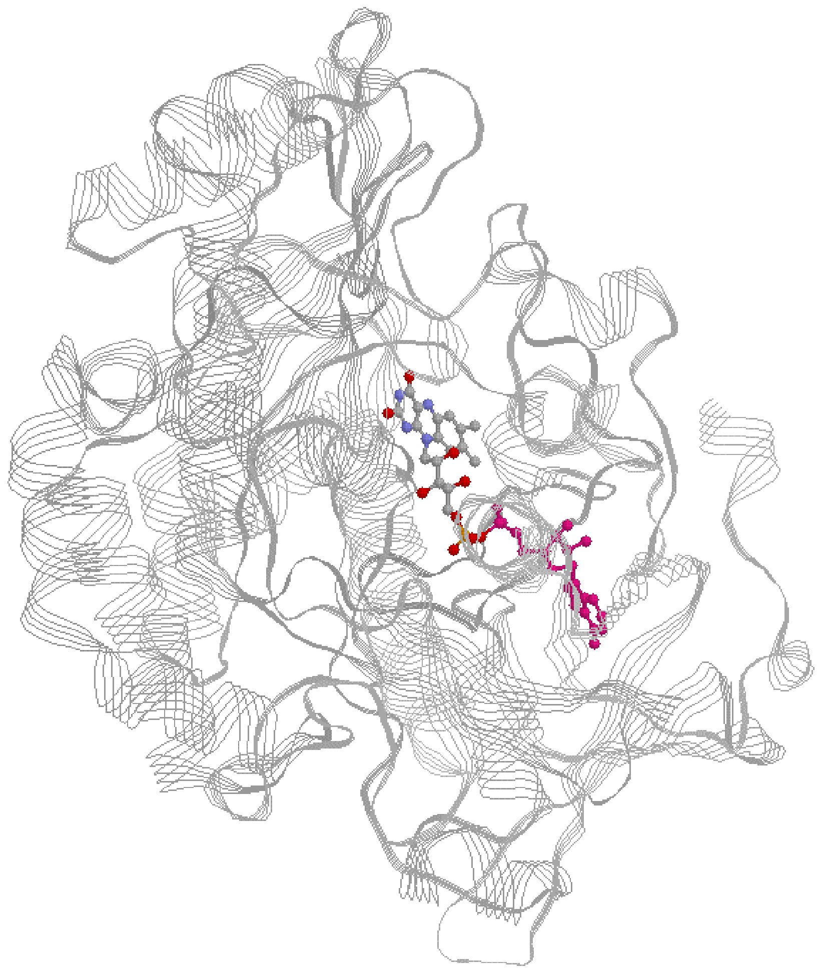

Figure 4.2**:** PDB structure of Glucose oxidase (GOx) – monomer as obtained from Swiss PDB viewer RASMOL. PDB ID: 1CF3[124] The protein part of the enzyme is represented as strands. The cofactor of the enzyme flavin adenine dinucleotide (FAD) is represented in ball and stick model.

Physical properties of GOx: Bentley has reviewed the general properties of the enzyme.[125]

(i) *Molecular weight*: ~160 kDa[121]

(ii) *Isoelectric point*: 4.2

(iii) *Solubility*: The protein is readily soluble in 0.1 M potassium phosphate at pH 7.0 giving a clear yellow solution.

(iv) *Diffusion coefficient*: The diffusion coefficient of the holoenzyme in 0.1 M NaCl is 4.94×10^{-7} $cm^2.s^{-1}$.

(v) *Stability*: Dry preparations are stable for years when stored cold. Solutions are reasonably stable under a variety of conditions.

(vi) *Oxidation-reduction potential*: The formal redox potential of GOx is reported as –380 mV vs SCE at pH 7.[126,127]

Functional properties of GOx: Glucose oxidase catalyses the electron transfer from glucose to oxygen with the production of gluconic acid and hydrogen peroxide.

(i) *Reaction mechanism*: A mechanism for the whole reaction with individual rate constants in a pH dependent scheme[128] has been proposed from a number of steady state and transient state kinetic analysis.[129] The catalytic cycle can be divided into two half reactions. In the first half reaction GOx catalyses the oxidation of β-D-glucose to δ-glucanolactone, which is subsequently hydrolyzed non-enzymatically to gluconic acid. The FAD of GOx is reduced to $FADH_2$.

$$\beta\text{-D-glucose} + \text{GOx-FAD} \Leftrightarrow \text{GOx-FADH}_2 + \delta\text{-glucanolactone} \quad (4.1)$$

In the second half-reaction the FAD in GOx is oxidized back by the reduction of molecular oxygen to H_2O_2.

$$\text{GOx-FADH}_2 + O_2 \rightarrow \text{GOx-FAD} + H_2O_2 \quad (4.2)$$

Various mediators can substitute molecular oxygen in the second half-reaction.

(ii) *Substrate specificity*: The enzyme shows a very high degree of specificity for β-D-glucose though 2-deoxy-D-glucose, D-mannose and D-fructose are also oxidized, the reaction proceeds at a much reduced rate.[130] Although very specific with regards to the reducing substrate, glucose oxidase shows a relatively high degree of flexibility with regards to the second substrate, i.e. the electron acceptor (oxygen). Thus, many inorganic redox couples and organic dyes have been successfully utilized as electron sinks for the enzyme-catalyzed oxidation of glucose.

(iii) *Inhibitors*: The enzyme reaction is inhibited by some glucose analogues such as 2-deoxy-D-glucose.

(iv) *Optimum pH*: 5.5 with broad range 4 – 7.[128,131]

(v) *Enzyme kinetics*: The Michealis constant depends on the degree of oxygen saturation (oxygen partial pressure). It has been reported that the enzyme shows a K_m of 33 mM for glucose in phosphate buffer at pH 5.6 in air at 20°C.[132,133] The K_m value with molecular oxygen which can be considered as the second substrate was reported to be 0.25 mM. The turnover number of the enzyme is 337 s^{-1}.[134]

Many techniques such as fluorescence, chemiluminescence, electrochemistry and flow injection analysis have been used for the purpose of determining the glucose concentration.[135-141] Electrochemical biosensors based on electron transfer between an electrode and immobilized GOx is especially promising. Various methods have been used for this purpose. Several authors investigated ion selective electrodes incorporating GOx coupled with oxidative reactions catalyzed by horseradish peroxidase (HRP).[142] Disturbances by other HRP substrates restrict the applicability of the method. Amperometric glucose sensors allow a simple measuring regime and makes use of the advantages of Faradaic electrode processes, such as independence of buffer capacity, linear concentration dependence and high sensitivity in substrate measurement. Cosubstrate oxygen and the product hydrogen peroxide, which are electrochemically active are used in most of those sensors.[143,144] These techniques are not applicable for solutions with varying oxygen content since the oxygen probed detects sum of the oxygen consumption in the enzyme membrane and the change in the bulk solution. In cases where the sensor relies on the formation of H_2O_2, various interferences reduce the applicability of the sensor.

To circumvent these problems various other procedures were developed. First is the direct electron transfer from the enzyme active site to the electrode surface in presence of glucose. But this method was not quite successful because the redox center ($FAD/FADH_2$) is buried from the surface of the enzyme.[145] Hence freely diffusing redox mediators as well as natural mediator i.e., oxygen has been used to transfer electrons between the active site of the enzyme and the electrode.[13,146] A novel principle for accelerating the electron transfer has been the direct chemical modification of GOx by electron-mediating groups such as ferrocene derivatives, phenoxazine and phenothiazine derivatives.[147-149.] Molecular wiring of the enzyme to the electrode surface through the amino group of the adenine (of FAD) to enhance the electron transfer from the enzyme redox center to the electrode surface has also been reported.[150]

In the present study we have considered the applicability of redox dyes Nile blue A, Brilliant cresyl blue and Toluidine blue as electron mediators upon covalently binding to glucose oxidase. We have also studied the effect of various coupling reagents used to couple the dyes to the enzymes. The enhancement of the electrochemical response on using coupling reagents with long spacer arms is also studied.

4.2 MATERIALS AND METHODS

4.2.1 Materials

Glucose oxidase from *Aspergillus niger* is obtained from Serva, Fein Biochemica GmbH & Co. Nile blue A, dicyclohexylcarbodiimide (DCC) and glutaraldehyde are obtained from Sigma. Brilliant cresyl blue is obtained from Fluka, Toluidine blue from Aldrich Chemie, Poly(ethylene glycol) 400 diglycidylether (PEGDGE M.W. 400) from Polysciences Inc., and Sephadex G25 from Amersham Biosciences. Sodium dithionite is obtained locally and other chemicals from Merck. All chemicals used are of analytical grade. Buffers are prepared using water purified with a Milli-Q system and degassed before use.

4.2.2 Instrumentation

Uvikon Spectrophotometer 930 from Kontron instruments is used for the spectroscopic studies.

Electrochemical experiments are carried out using BAS 100A instrument with a three-electrode setup. Spectrographic graphite (SPGE) rod of 3.05 mm diameter and 13% porosity is used as the working electrode. KCl saturated calomel reference electrode and a gold counter electrode are used.

The Flow injection system consisting of a peristaltic pump (Gilson Miniplus 3), an injection pump (Lab Pro) and a flow-through electrochemical cell under three-electrode potentiostatic control (Zäta Electronic, Sweden) is used. Ag/AgCl (KCl saturated) served as the reference electrode, platinum as the counter electrode and spectrographic graphite as the working electrode.

4.2.3 Methodology

4.2.3.1 Covalent coupling of Glucose oxidase with the redox dyes using carbodiimide (DCC)

Aqueous solution 2 mM of the dye solutions are reduced using sodium dithionite. Drops of sodium thionite solution are added to the dye solution till it undergoes a colour change. 200 μl of 2 mM of DCC dissolved in ethanol is added to a mixture containing 200 μl of 0.15 mM glucose oxidase (dissolved in 0.1 M phosphate buffer of pH 7) and 200 μl of 2 mM of the reduced dyes. The coupling mixture is incubated overnight at room temperature before purifying the coupled enzyme from the uncoupled dye on a 20 ml Sephadex G25 column. 1 ml fractions of the eluate are collected discarding the initial 5 ml corresponding void volume and their absorbance at the λ_{max} of the oxidized dye and the reduced dye (315 nm) as well as at 280 nm (λ_{max} of GOx) and at 460 nm are recorded. Since the reduced dyes show high absorbance at 280 nm, the absorbance of glucose at the next maximum wavelength 460 nm is used to calculate the amount of GOx present in the coupled sample. The molar extinction coefficient of GOx at 460 nm is 28,200 $M^{-1}cm^{-1}$,[151] which is used for calculating the degree of coupling.

4.2.3.2 Covalent coupling of the redox dyes to glucose oxidase using glutaraldehyde

200 µl of 2 mM of glutaraldehyde is added to a mixture containing 200 µl of 0.15 mM glucose oxidase (dissolved in 0.1 M phosphate buffer of pH 7) and 200 µl of 2 mM of the reduced dyes. The coupling mixture is incubated at room temperature for 4 hours before purifying on the Sephadex gel. During this reaction the amino group of the dyes is cross-linked to the amino group of the basic amino acid residues present in the enzyme as shown in Fig. 4.3.

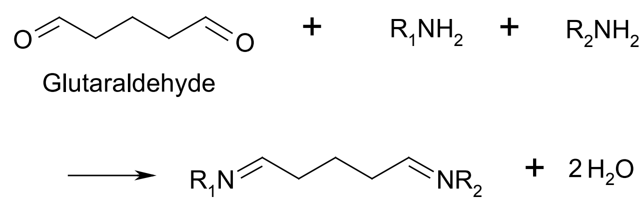

Figure 4.3: Covalent coupling of the dyes (R_2NH_2) to glucose oxidase (R_1NH_2) using glutaraldehyde. The maximum yield of the desired compound (with R_1 and R_2 at the two ends) cannot be greater than 50%.

Though the efficiency of coupling is not high using these concentrations, they reduce the amount of unwanted cross-linking of the dyes and the enzyme, which may form during the reaction as glutaraldehyde has two similar reactive groups. Glutaraldehyde is susceptible for polymerization in presence of oxygen and though the experiments are carried out using degassed solutions a possibility of polymerization of the reagent is always present. In such a case the dyes would be linked to the enzyme with a longer spacer arm between them, which, may affect the electrochemical studies.

4.2.3.3 Covalent coupling of the redox dyes to glucose oxidase using PEGDGE

200 µl of 2 mM of PEGDGE is added to a mixture containing 200 µl of 0.15 mM glucose oxidase (dissolved in 0.1 M phosphate buffer of pH 7) and 200 µl of 2 mM of the reduced dyes. The coupling mixture is incubated overnight at room temperature before purifying the coupled enzyme from the uncoupled dye on the Sephadex G25 column. During this reaction the amino group of the dyes is cross-linked to the amino group of the basic residues of the enzyme with a long spacer arm as shown in Fig. 4.4. The coupling efficiency using the concentrations of the reactants used may not be high but the protocol has been standardized to reduce cross reactivity among the dyes and the enzyme as the coupling reagent contains two identical similar reactive groups as in the case of glutaraldehyde.

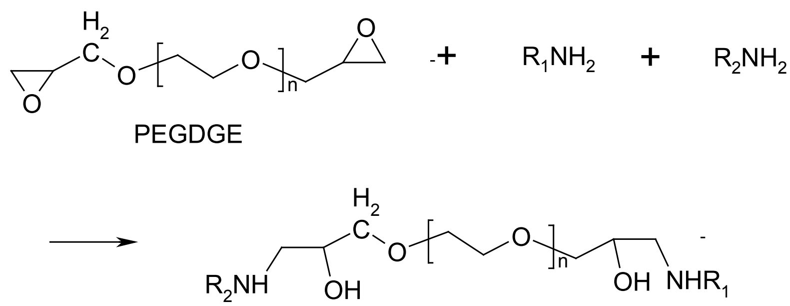

Figure 4.4: Covalent coupling of the dyes (R_2NH_2) to glucose oxidase (R_1NH_2) using PEGDGE. (n is ~6). The maximum yield of the desired compound (with R_1 and R_2 at the two ends) cannot be greater than 50%.

4.2.3.4 Electrochemical studies on Glucose oxidase coupled with dyes.

5 µl of ~5 µM of the coupled sample is placed on a spectrographic graphite electrode of 3.05 mm diameter, polished on wet fine emery paper (Tufback Durite, P1200) and allowed to dry overnight at 4ºC. This irreversibly adsorbs the enzyme to a graphite electrode surface. Cyclic voltammetry of

the adsorbed samples after rinsing with water to remove the unadsorbed sample are recorded in absence and presence of 5 mM glucose. A 15 ml electrochemical cell containing 0.1 M phosphate buffer of pH 5.5 as the electrolyte is used. The solution is deaerated using Argon gas bubbling before carrying out the experiments.

4.2.3.5 Amperometric response of GOx coupled with the dyes to glucose using flow injection analysis setup

Degassed 0.1 M phosphate buffer of required pH is used as the carrier solution. Volume of the analyte (glucose) injected is 50 µl. Experiments are carried out with a flow rate of 0.2 ml/min. Amperometric response of the GOx coupled with the dyes adsorbed on the graphite working electrode, for the injection of the glucose into the flow cell is monitored. Current intensities are measured as peak heights and the average of the heights of three injections is represented along with the standard error. The peak height is measured from the baseline to the peak manually.

4.3 RESULTS AND DISCUSSION

4.3.1 Degree of coupling

Since the coupled enzyme elutes earlier than the uncoupled dye due to its higher molecular weight, the fraction, which first elutes with maximum absorbance at λ_{max} of the dye and at 460 nm represents the coupled enzyme. Fig. 4.5 shows the elution profile of one of the coupling reaction mixture. A simultaneous increase in the absorbance at the λ_{max} of the dye (625 nm for native Nile blue A and 315 nm for the reduced dye) and the λ_{abs} of the enzyme used for calculating the degree of coupling (460 nm) is observed in the third fraction indicating the elution of the coupled sample.

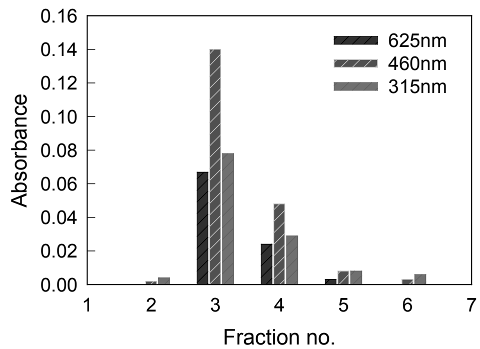

Figure 4.5: Elution profile of the coupling reaction mixture of Nile blue A and glucose oxidase using PEGDGE. A simultaneous increase in the absorbance at the λ_{max} of the dye (625 nnm and 315 nm) and at 460 nm (λ_{abs} for GOx) is observed in fraction 3 indicating the elution of the coupled sample.

The degree of coupling (*DOC*) i.e., number of dye molecules per protein molecule, is calculated for all the coupled samples using the formula,

$$DOC = \frac{A_{\max} \times MW}{[protein] \times \varepsilon_{dye}} \tag{4.3}$$

where $A_{\max}$ is the absorbance at $\lambda_{\max}$ of the dye, MW - molecular weight of the protein, [*protein*] - protein concentration in mg/ml and ε_{dye} – molar extinction coefficient of the dye.

Fig. 4.6 shows the comparative degree of coupling of GOx with the dye molecules using different coupling reagents. Since the absorbance of the dye changes on binding to the enzyme the degree of coupling is not absolute and cannot be used for comparative study between different dye molecules. But the comparative degree of coupling using different coupling reagents is informative. It is observed that the degree of coupling using any of the coupling reagents is identical. In case of Toluidine blue the degree of coupling is much better with DCC coupling reagent than with other coupling reagents.

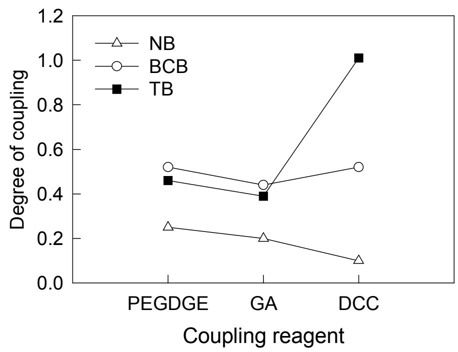

Figure 4.6: Schematic representation of the degree of coupling of GOx with Nile blue A (NB), Brilliant cresyl blue (BCB) and Toluidine blue (TB) using PEGDGE, Glutaraldehyde (GA) and DCC coupling reagents. It reveals that the degree of coupling is identical using any of the coupling reagents. The DOC of TB with GOx is higher when DCC is used when compared to GA and PEGDGE.

4.3.2 Electrochemical studies on GOx coupled with the dyes

Cyclic voltammetry is carried out on the enzyme coupled with the dyes immobilized on the graphite electrode. Fig. 4.7 shows the cyclic voltammogram of a blank or naked graphite electrode before immobilising the enzyme.

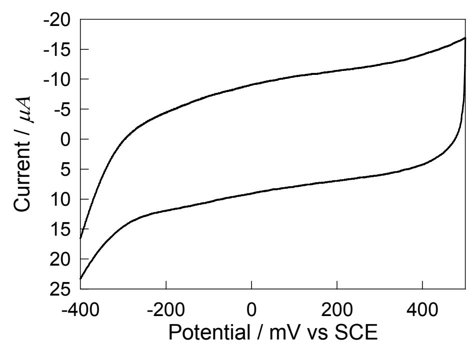

Figure 4.7: Cyclic voltammogram of naked graphite electrode. Forward Scan direction: -400 mV to 450 mV. Scan rate: 100 mV/sec

All the coupled samples are electroactive in nature irrespective of the coupling reagent used. A shift of the formal potential of the dyes to positive potentials on binding to the enzyme and after adsorbing on to the electrode surface is observed (Fig. 4.8). This is due to the derivatization of the amino group in the side chain of the dyes.[70] GOx binds to the amino group of the dyes during the coupling process resulting in a positive shift of the redox potential.

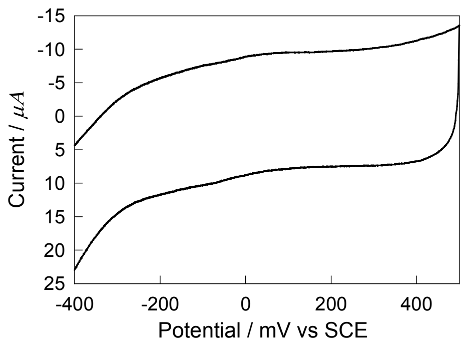

Figure 4.8: Cyclic voltammogram of adsorbed GOx coupled with Nile blue A using glutaraldehyde. Forward Scan direction: -400 mV to 450 mV. Scan rate: 100 mV/sec. An oxidation hump is observed around 44 mV and a reduction hump around –74 mV.

A strong adsorption of the dye coupled enzyme to the electrode is observed with negligible effect on the peak current even after multiple scans. ΔE_p for the adsorbed dye coupled GOx is observed to be > 59 mV indicating kinetic restrictions for electron transfer. But since negligible increase in the ΔE_p with scan rate is observed it is concluded that the electron transfer is relatively facile.

Fig. 4.9 shows the cyclic voltammograms of GOx coupled with Nile blue A using DCC coupling reagent in absence and presence of the substrate glucose. In presence of glucose, the enzyme gets reduced and in turn reduces Nile blue A which is oxidized at the electrode surface. An increase in the oxidation current of ~10 nA is observed in presence of 5 mM glucose.

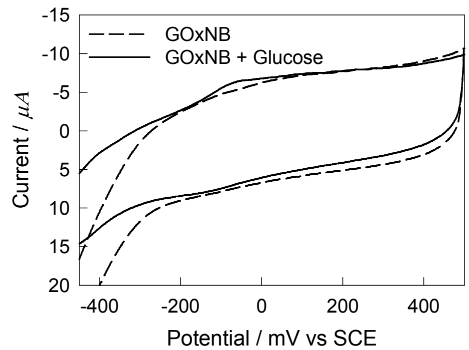

Figure 4.9: Cyclic voltammograms of adsorbed GOx coupled with Nile blue A using DCC in absence and presence of 5 mM glucose. Scan rate: 50 mV/sec. An increase in the oxidation current of ~10 nA is observed in presence of 5 mM glucose.

4.3.3 Amperometric response of GOx coupled with the dyes for glucose - FIA

When glucose is injected into the carrier stream, it reaches the working electrode surface where it is gets oxidized to δ-glucanolactone catalysed by GOx immobilized on the working electrode surface. The cofactor of the enzyme gets reduced to $FADH_2$, which in turn gets oxidized by reducing the covalently bound mediators (dyes). The dyes are regenerated back by oxidation at the electrode surface, which results in an increase in the current indicated by a peak on the output chart. Fig. 4.10 shows the response of 50 picomoles/cm^2 of GOx coupled with the dyes using different coupling reagents adsorbed on the graphite working electrode. 50 µl of 5 mM glucose is injected into the flow cell. It is observed that dyes coupled to GOx using PEGDGE as the coupling reagent transfer the electrons from the active site to the electrode more efficiently than the dyes coupled using glutaraldehyde or DCC coupling reagent. This might be attributed to the long chain of the reagent, which makes the active site more accessible to the bound mediator. Though the degree of coupling of Toluidine blue to GOx using DCC is relatively higher, the electrochemical response is less than that observed for

GOx coupled using PEGDGE. This also can be attributed to the effect of the long chain of PEGDGE.

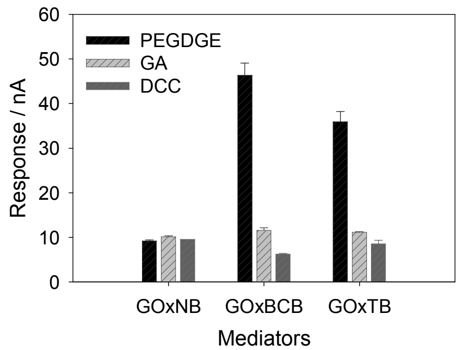

Figure 4.10: Relative response shown for 50 µl of 5 mM glucose at -100 mV by adsorbed GOx coupled with dyes Nile blue A (GOxNB), Brilliant cresyl blue (GOxBCB) and Toluidine blue (GOxTB) using coupling reagents PEGDGE, Glutaraldehyde (GA) and DCC.

The response shown by the coupled samples where glutaraldehyde is used as the coupling reagent might be affected due to the polymerization of glutaraldehyde in aqueous solution.[152] This would lead to enhanced electrochemical response than when the polymerization is absent since the distance between the dye and the protein molecule is increased leading to the flexibility of the dye near the active site region.

It is observed that Brilliant cresyl blue and Toluidine blue whose formal potentials (-195 mV and –208 mV respectively)[57] are higher than Nile blue A (-361 mV) mediate the electron transfer from the active site of the enzyme to the electrode better. This shows that the redox potential of the mediator also plays an important role. Higher the redox potential of the mediator better is the electron transfer in case of GOx.[145]

Effect of working potential: Fig. 4.11 shows the dependence of the response of enzyme coupled with the dyes on the applied working potential in presence of 50 µl of 5 mM glucose. Maximum response is observed at -100 mV for enzymes coupled with any of the three dyes, which is more pronounced in case of GOx coupled with Brilliant cresyl blue. The reason for the decrease in the response at higher potentials is unknown.

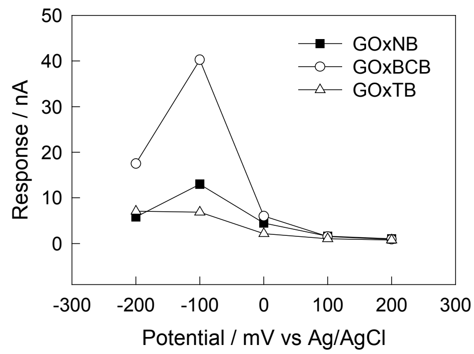

Figure 4.11: Response of GOx coupled with Nile blue A (GOxNB), Brilliant cresyl blue (GOxBCB) and with Toluidine blue (GOxTB) for 50 µl of 5 mM glucose. Optimum response is observed at –100 mV.

A comparative study of the response of the enzyme electrodes coupled with different dyes cannot be made using these results, as they are not samples coupled using the same coupling reagent and also the amount of enzyme immobilized is not equal.

Effect of pH: Maximum response is observed in the pH range of 5-6 (Fig. 4.12). Above pH 6 a decrease in the response is observed for enzyme coupled with Brilliant cresyl blue and Toluidine blue. GOx coupled with Nile blue A appears to be more stable to a change in pH in the range of 5-7.

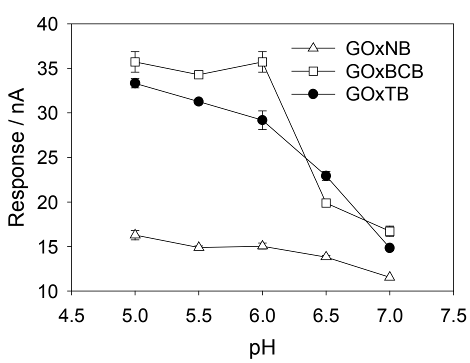

Figure 4.12: Response of GOx coupled with Nile blue A (GOxNB), Brilliant cresyl blue (GOxBCB) and with Toluidine blue (GOxTB) using PEGDGE, for 50 µl of 5 mM glucose at –100mV working potential. Optimum response is observed in the pH range of 5-6.

This shows that the enzymatic properties of glucose oxidase are not much affected by the covalent coupling of the dyes to the enzyme since native glucose oxidase shows an optimum activity around pH 5.5 (vide supra)

<u>*Effect of varying concentration of the analyte*</u>: Fig. 4.13 shows the flow injection response of 48 picomoles/cm^2 of the dye coupled enzyme adsorbed onto the electrode surface in presence of varying concentration of glucose. Assuming 100% adsorption, since 5 μl of 3.4 μM is kept for adsorption on an electrode of 0.35 cm^2 effective surface area, the final coverage area of the enzyme on the electrode would be 48 picomoles/cm^2.

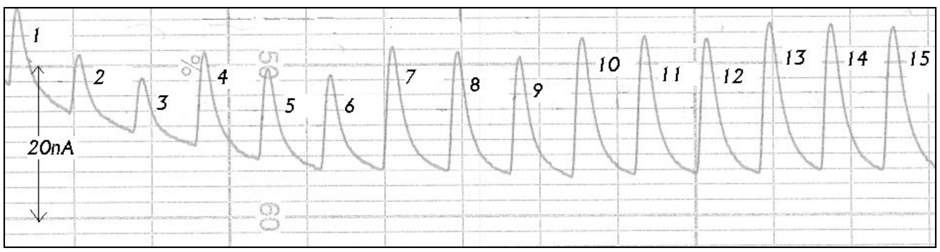

Figure 4.13: Flow injection output of glucose oxidase coupled with Toluidine blue using PEGDGE for varying concentration of glucose injected. Peaks 1-3: 2 mM glucose, 4-6: 4 mM glucose, 7-9: 6 mM glucose, 10-12: 8 mM and 13-15: 10 mM glucose.

A linear response for the injection of glucose upto ~6 mM concentration is observed (Fig. 4.14). Above 6 mM concentration of the substrate (glucose) the response is more or else constant suggesting the saturation of the enzyme with the substrate, which is a general trend of an enzyme-substrate reaction.

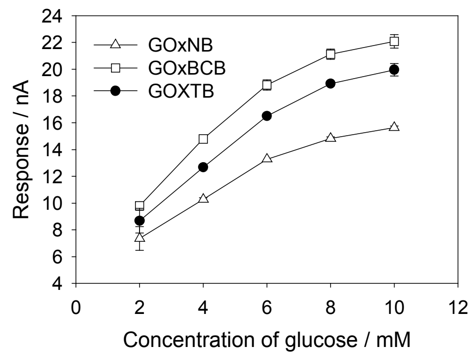

Figure 4.14: Response of GOx coupled with Nile blue A (GOxNB), Brilliant cresyl blue (GOxBCB) and Toluidine blue (GoxTB) using PEGDGE for the injection of 50 µl glucose of varying concentration.

Higher concentrations of the substrate can be detected by dilution. Thus this system can be used for qualitative and quantitative detection of glucose in a given sample.

4.4 CONCLUSIONS

The coupled samples are electroactive irrespective of the coupling reagent used. A shift of the formal potential of the dyes to positive potentials on binding to the enzyme and after adsorbing on to the electrode surface indicates the derivatization of the amino group present in the side chain of the dyes indicating that the dyes have been covalently bound to the enzyme.

A strong adsorption of the modified enzyme to the electrode surface is observed indicated by negligible effect on the peak current even after repetitive scans. This shows that the enzyme electrodes are quite stable with negligible leaching. ΔE_p of > 59 mV indicates that the electron transfer is slow but as the increase in ΔE_p with scan rate is negligible, it can be concluded that the electron transfer might not be very fast but is relatively facile.

GOx coupled with the dyes using PEGDGE as the coupling reagent transfers the electrons from the active site to the electrode more efficiently than the dyes coupled using glutaraldehyde or DCC. This is attributed to the long chain of the reagent, which reduces the electron transfer distance and enhances the electrochemical activity of the enzyme.

Brilliant cresyl blue and Toluidine blue of higher redox potentials are better electron mediators for glucose oxidase than Nile blue A which has comparatively low redox potential. Higher the redox potential of the mediator better is the electron transfer in case of GOx.

Linear response of the enzyme electrode to the concentration of glucose is observed and therefore the sensor can be used not only qualitatively but also quantitatively.

GOx coupled with Brilliant cresyl blue using PEGDGE shows better response than those coupled with Nile blue A and Toluidine blue. Added to the above characteristics, since the enzyme electrodes are appreciably stable for over a week and the leaching of the enzyme from the electrode surface is negligible this setup can be efficiently used as a glucose biosensor.

SUMMARY

SUMMARY

Redox dyes have a dual advantage of spectroscopic and electrochemical detection. We have studied the use of redox dyes as non-diffusional electron mediators in electrochemical biosensors.

The major conclusions of our study are-

1. The dyes maintain their redox characteristics even after binding to the redox proteins and thus help in the electrochemical detection of proteins, which cannot be efficiently detected electrochemically.

2. Though the exact residue(s) on the enzyme to which the dye is coupled is not known, as the coupling procedure used is not specific, covalently coupled dyes efficiently transfer the electrons between the active site of the enzymes and the electrode surface, which otherwise is hindered by the protein shell.

3. The optimum potential for the enzyme electrode kinetics is reduced on covalently coupling the enzyme with the dyes. This overcomes the problem of various interferences at higher potentials.

4. The redox potential of the dye plays an important role in non-diffusion mediated electron transfer. We have observed that higher the redox potential of the mediator better the electrocatalytic effect of the dye bound to glucose oxidase.

5. Use of a spacer arm between the dye and the enzyme such as diaminohexane or a coupling reagent with spacer arm such as

PEGDGE enhances the electrocatalytic effect of the redox dyes as the spacer arm is flexible and so the dye molecules can easily take up or give electrons near the active site region as well as the distance between the active site of the enzyme and the electrode surface is reduced because of the spacer arm.

6. The dye coupled enzymes show linear response to the substrate concentration and therefore can be effectively used for quantitative analysis.

7. Safranine O coupled to HRP mediates the electron transfer better than Neutral red coupled to HRP, along with lowering the required working potential and therefore with further optimizations such as use of a spacer arm to bridge the dye and the enzyme, this setup can be efficiently used for developing a successful hydrogen peroxide biosensor.

8. GOx coupled with Brilliant cresyl blue using PEGDGE shows better response than GOx coupled with Nile blue A and Toluidine blue and since there is negligible leaching of the enzyme from the electrode surface added to the stability of the enzyme electrode for over a week, this setup can be efficiently used as a glucose biosensor.

REFERENCES

1. L.C. Clark, *Biosensors-fundamentals and applications*, (Eds. A.P.F. Turner, I. Karube and G. Wilson), Oxford University Press (1989) 3-12.
2. L.D. Browers, *Anal. Chem*. 58 (1986) 513A-530A.
3. M. Thompson and U.L. Krull, *Anal. Chem*. 63 (1991) 393A-405A.
4. P.J. Mareck, Kierstan and M.P. Coughlan, *Protein immobilization – Fundamentals and Application*, (Eds. R.F. Taylor), Marcell Dekker Inc., New York (1991).
5. J.M.S. Cabral and J.F. Kennedy, *Protein immobilization – Fundamentals and Applications*, (Eds. R.F. Taylor), Marcell Dekker Inc., New York (1991).
6. J.M. Nelson and E.J. Griffin, *J Amer. Chem. Soc*. 38 (1916) 1109-1115.
7. P.W. Carr and L.D. Bowers, *Immobilised Enzymes in Analytical and Clinical Chemistry*, Wiley, New York (1980).
8. G.J. Bastians, *Chemical sensors*, (Eds. J.E. Edmonds), Blakie, Glasglow (1988).
9. F. Scheller, F. Scbert *et al*., *Analyst* 114 (1989) 653-662.
10. R.K. Kobos, *Ion selective electrodes in analytical chemistry*, (Eds. H. Fresier), Vol 2, Plenum-New York (1980).
11. Frieder Scheller and Florian Schubert, *Fundamentals of biosensors in "Biosensors"*, Elsevier Science Publishers, New York (1982) 24-33.
12. Keith Wilson and John Walker, Electrochemical techniques in *"Practical Biochemistry"*, Cambridge University Press (2000) 739-742.
13. A.E.G. Cass, G. Davis *et al*., *Anal.Chem.* 56 (1984) 667.
14. A.L. Ghindilis, P. Atanasov and E. Wilkins, *Electroanalysis*, 9 (1997) 661.
15. D.J.G. Ives and E.J. Jans, *General and theoretical introduction: Reference electrodes*, Academic press, New York (1961) 1-70.
16. Samuel P. Kounaves, *Voltammetric techniques in "Handbook of instrumental techniques for Analytical Chemistry*" 717-719. (http://www.prenhall.com/settle/chapters/ch37.pdf).

17. M.J. Honey church and G.A. Rechnitz, *Electroanalysis* 10 (1998) 285.

18. Allen J. Bard and Larry R. Faulkner, *Electrochemical Methods-Fundamentals and Applications*, John Wiley & sons, USA (1980) 522.

19. Peter T. Kissinger and William R. Heineman, *Laboratory Techniques in Electroanalytical Chemistry*, Marcal Dekker Inc., New York (1996) 150-152.

20. J. Ruzicka and E.H. Hansen, *Anal.Chim. Acta* 78 (1975) 145-157.

21. Bo Karlberg and Gil E. Pacey, *Flow Injection Analysis*, Elsevier Science Publishers, Netherlands (1989) 29-64.

22. D.R. Thévenot, K. Toth, *et al*., *Biosens. Bioelectron*. 16 (2001) 121-131.

23. L.C. Clark Jr. and C. Lyons, *Ann. Ny Acad. Sci*. 102 (1962) 29.

24. J.A. Cowan and H.B. Gray, *Chem. Scripta* 28A (1988) 21-26.

25. R.A. Marcus and N. Sutin, *Biochem. Biophys. Acta* 811 (1985) 265.

26. Heller, *Acc. Chem. Res*. 23 (1990) 128-134.

27. W. Schuhmann, *Biosens. Bioelectron*. 10 (1995), 181-193.

28. P.N. Bartlett, P. Tebbutt and R.C. Whitaker, *Prog. Reaction Kinetics* 16 (1991) 55-155.

29. J. Wang, *J. Pharm. Biomed*. Anal. 19 (1999) 47-53.

30. Y. Yamazaki and H. Maeda, *Agricult. Biol. Chem*. 46 (1982) 1571-1581.

31. I. Willner, E. Katz *et al*., *J. Chem. Soc., Perkin Trans.* 2 (1998) 1817-1822.

32. I. Willner, A. Riklin *et al*., *Adv. Mater*. 5 (1993) 912-915.

33. B. Shoham, Y. Migron *et al*., *Biosens. Bioelectron*. 10 (1995) 341-352.

34. F. Mizutani and M. Asai, Bull. *Chem. Soc. Jpn*. 61 (1988) 4458-4460.

35. P. Janda and J. Weber, *J. Electroanal. Chem*. 300 (1991) 119-127.

36. V.J. Razumas, A.V. Gudavicius and J.J. Kulys, *J. Electroanal. Chem*. 198 (1986) 81-87.

37. F. Patolsky and G. Tao *et al., J. Electroanal. Chem.* 454 (1998) 9-13.

38. A. Narvaez, E. Dominguez *et al*. *J. Electroanal. Chem*. 430 (1997) 217-233.

39. Y. Degani and A. Heller, *J. Phys. Chem*. 91 (1987) 1285-1289.

40. I. Willner and E. Katz, *Angew. Chem., Int. Ed*. 39 (2000) 1180-1218.

41. W. Schuhmann, T.J. Ohara, *et al*., *J. Am. Chem. Soc*. 113 (1991) 1394-1397.

42. Y. Degani and A. Heller, *J. Am. Chem. Soc*. 110 (1988) 2615-2620.

43. G. Beckars, R.J. Berzborn and H. Strotmann, *Biochim Biophys Acta* 1101 (1992) 97-104.

44. L. Finar, Dyes in *"Organic Chemistry"*, Longmans, Green &Co Ltd, London (1969) 821-829.

45. Samuel Glasstone, Electrochemistry in "*Text book of Physical Chemistry"*, Ed. 2, Macmillan India Press, Madras (1976) 952-953.

46. I. Taniguchi, S. Miyamoto *et al*., *J. Electroanal. Chem*. 240 (1988) 333-339.

47. Y.A. Aleksandrovskii, L.V. Bezhikina and Y.V. Rodionov, *Biokhimiya* 46 (1981) 708-716.

48. C. Iwakura, Y. Kajiya and H. Yoneyama, *J. Chem. Soc*., Chem. Commun. (1988) 1019-1020.

49. Y. Kajiya, H. Sugai et al, *Anal. Chem*. 63 (1991) 49-54.

50. A.E.G. Cass, G. Davis, *et al*., *Charge and Field Effects in Biosystems*, (Eds. M.J. Allen, P.N.R. Usherwood) Abacus (1984) 475-484.

51. N.C. Foulds and C.R. Lowe, *J. Chem. Soc., Faraday Trans*. 1 82 (1986) 1259-1264.

52. J.J. Kulys and R.A. Vidziuaite, *Anal. Lett*. 16 (1983) 197-207.

53. Y. Kajiya, R. Tsuda and H. Yoneyama, *J. Electroanal. Chem*. 301 (1991) 155-161.

54. T. Matsue, N. Kasai *et al*., *J. Electroanal. Chem*. 300 (1991) 111-118.

55. T. Ohara, R. Rajogopalan and A. Heller, *Anal. Chem*. 66 (1994) 2451.

56. I. Willner, V. Heleg-Shabtai *et al*., *J. Am.Chem. Soc*. 118 (1996) 10321.

57. Edmund Bishop, Oxidation –Reduction Indicators in "*Indicators*", Ed. 1, Pergamon Press, Oxford (1972) 490-510.

58. Susan Budavari, *The Merck Index*, Ed. 12, Merck & Co., Inc., Whitehouse Station, NJ, USA (1996).

59. Edward Gurr**,** *Synthetic dyes in biology, medicine and chemistry*, Academic Press, London, England (1971).

60. J. Dacie and S. Lewis, *Practical haematology*, Churchill Livingstone, London (1966) 1995.

61. B. Cohen and P.W. Priesler, *Public Health Reports (U.S),* Suppl. No. 92 (1931).

62. Z. Wang, Z. Zhang *et al*., *Spectrochim Acta A Mol Biomol Spectrosc*. 59 (2003) 949-56.

63. Y. Cao and X.W. He, *Spectrochim Acta A Mol Biomol Spectrosc*.54A (1998) 883-92.

64. C.W. Lin, J.R Shulok et al., *Cancer Research* 51 (1991) 2710-2719.

65. D.K. Chelvanayagam and L.D. Beazley *J Neurosci Methods* 72 (1997) 49-55.

66. S. Bauminger and M. Wilchek, *Methods Enzymol*. 70 (1980) 151-159.

67. J.M. Tedder, A. Nechvatal *et al*., *Basic organic chemistry-Amino-acids and proteins*. John Wiley & Sons, London (1972). 305-342.

68. W.M. Clark, *Oxidation-Reduction potentials of Organic Systems*, Williams and Wilkins, Baltimore (1960).

69. E. Laviron, *Electroanalytical Chemistry*, Vol 12 (Eds: A.J. Bard), Marcel Dekker, New York (1982) 53-157.

70. Björn Persson and Lo Gorton, *J. Electroanal. Chem*., 292 (1990) 115-138.

71. Allen J. Bard And Larry R. Faulkner, *Electrochemical Methods-Fundamentals and Applications*, John Wiley & sons, USA (1980) 190-194.

72. Donald T. Sawyer and Julian L. Roberts, Jr, Controlled potential methods in "*Experimental Electrochemistry for Chemists*", John Wiley & Sons, U.S.A, (1974).

73. L. T. Kubota and Lo Gorton, *Electroanalysis*, 11 (1999) 719-728.

74. B.R. Horrocks, D. Schmidtke *et al*., *Anal Chem*. 65 (1993) 3605-3615.

75. E.A.H. Hall, *Biosensors*, Open University Press, Milton Keynes (1990).

76. L.C. Clarc, *Methods Enzymology* 56 (1979) 448.

77. J. Wang, N. Naser *et al*., *Anal. Chem*. 64 (1992) 1285.

78. H.Y. Liu, T.L. Ying *et al*., *Anal. Chem*. 344 (1997) 187.

79. N.C. Foulds and C.R. Lowe, *Anal. Chem*. 60 (1988) 2473.

80. T. Tatsuma, Y. Okawa, and T. Watanabe, *Anal. Chem*. 61 (1989) 2352.

81. G. Jonsson and L. Gorton, *Electroanalysis* 1 (1989) 465.

82. G.J. Peterson, *Electroanalysis* 3 (1991) 741.

83. C. Ruan, F. Yang *et al*., *Anal. Chem*. 70 (1998) 1721.

84. Y. Xiao, H. Ju and H. Chen, *Anal. Chim. Acta* 391 (1999) 299.

85. T. Lotzbeyer, W. Schuhmann, and H.-L. Schmidt, *Bioelectrochem. Bioener.* 42 (1997) 1.

86. M. Mukai, S. Nagano *et al*., *J. Am. Chem. Soc*. 119 (1997) 1758.

87. D. Keilin and E.F. Hartee*, J. Biochem*. 49 (1951) 88-97.

88. H. Theorell, *Enzymologia* 10 (1942) 250-252.

89. M.L. Shannon, E. Kay and J.Y. Lew, *J. Biol. Chem*. 241 (1966) 2166-2172.

90. A.C. Mehly, Plant peroxidases in "*Methods in enzymology*", (Eds. S.P. Colowick, N.O. Kaplan), Vol 2, Academic Press, New York (1955) 801-813.

91. A.C. Mehly, Biochim. *Biophys. Acta*. 81 (1952) 1-17.

92. H.A. Harbury, *J Biol Chem*. 1957 (2) 1009-1024.

93. G.I. Berglund, G.H. Carlsson *et al*., *Natur*e 417 (2002) 463-468.

94. B. Chance, *The Enzymes*, (Eds. J.B. Sumner and K. Myrback), Vol 2, Part 1 ,Academic Press, New York (1951).

95. B. Chance, *Advances in enzymology*, (Eds. F.F. Nord) Vol 12, Interscience Publishers (1951) 153-190.

96. J. Dawson, *Science* 240 (1988) 433.

97. S.L. Newmyer and P.R. Ortiz deMontellano, *J. Bio. Chem*. 270 (1995) 19430-19438.

98. M. Sivaraja, D.B. Goodin and B.M. Hoffman, *Science* 245 (1989) 738-740.

99. H. Yamada and I. Yamazaki, Arch. *Biochem. Biophys*. 165 (1974) 728-738.

100. A. Maehly and B. Chance, *Methods Biochem Anal* 1 (1954) 357.

101. J. Chmielnicka, P. Ohlsson *et al*., *FEBS Lett* 17 (1971) 181.

102. M. Morrison and G. Bayse, *Peroxidase-Catalyzed Reactions, Oxidases and Related Redox Systems*, (Eds. T. King, H. Mason, and M. Morrison), Univ Pk Press, Baltimore, MD, USA (1973) 375.

103. H. Theorell, *The Enzymes*, (Eds.J. Sumner and K. Myrback), Academic Press, NY (1951) 397.

104. H.U. Bergmeyer and M. Grass1, H.E. Walter, *Methods of Enzymatic analysis*, Ed. 3, Vol II, Verlag Chem, Weinheim, (1983) 267-268.

105. J. Green and H.A.O. Hill, *Faraday Trans*. 182 (1986) 1237.

106. Chunhai Fan, Haiyan Wang *et al*., *Anal. Sci*. 17 (2001) 273-276.

107. T. Yao, M. Sato *et al*., *Anal. Biochem*. 149 (1985) 387.

108. A.A. Shul'ga and T.D. Gibson, *Anal.Chim Acta.* 296 (1994) 163.

109. U. Wollenberger, J. Wang *et al*., *Bioelectrochem. Bioenerg*. 26 (1991) 287.

110. W.O. Ho, D. Athey *et al*., *J. Electroanal. Chem*. 351 (1993) 185.

111. T. Ruzgas, L. Gorton *et al*., *J. Electroanal. Chem*. 391 (1995) 41.

112. A. Heller, *J. Phys. Chem*. 96 (1992) 3579-3587.

113. Hui Yao, Nan Li *et al*., *Sensor*s 5 (2005) 277-283.

114. U. Korell and U.E. Spichiger, *Anal.Chem*. 66 (1994) 510-515.

115. Allen J. Bard and Larry R. Faulkner, *Electrochemical Methods-Fundamentals and Applications,* John Wiley & sons, USA (1980) 525-527.

116. B. Szajani, A. Molnar *et al*., *Appl. Biochem. Biotechnol*, 14 (1987) 37-47.

117. R. Wilson, and A.P.F. Turner, Biosens. Bioelectr. 7 (1992) 165-185.

118. M. Röhr, C.P. Kubicek and J. Kominek, *Biotechnology*, (Eds. H.-J. Rehm and G. Reed) Vol. 3, Verlag Chemie, Weinheim (1983) 455-465.

119. A. Crueger and W. Crueger, *Biotechnology*, (Eds. H.J. Rehm and G.Reed) Vol. 6A, Verlag Chemie, Weinheim (1984) 421-457.

120. J.O'Malley, and Weaver, *J Biochem* 11 (1972) 3527.

121. H. Tsuge, O. Natusaki and K. Ohashi, *J Biochem* 78 (1975) 835.

122. W. Schumann and H.L. Schmidt, *Adv. Biosen*. 2 (1992) 79.

123. H.J. Hetcht, H.M. Kalisz *et al*., *J. Biol. Chem*. 229 (1993) 153.

124. G. Wohlfahrt, S. Witt *et al*., *Acta Crystallogr., Sect.D* 55 (1999) 969-977.

125. R. Bentley *The Enzymes*, (Eds P. Boyer, H. Lardy, and K. Myrback) 2nd Ed, Academic Press, NY (1963) 567.

126. B.R. Eggin. *Biosensors-An Introduction*, John Wiley, New York (1997).

127. E.I. Iwuoha, M.R. Smyth and J.G. Vos, *Electroanalysis* 6 (1994) 982.

128. H.J. Bright and M. Appleby, *J. Biol. Chem*. 244 (1969) 3625-3634.

129. H. Bright, and D. Porter, *The Enzymes*, (Eds. P. Boyer) Ed. 3, Academic Press, NY (1975) 421.

130. R. Bentley, *Methods in Enzymology*, (Eds. W. Wood), Academic Press, NY (1966) 86.

131. M. Weibel and H. Bright, *J Biol Chem* 246 (1971) 2734.

132. F. Scheller and F. Schubert, *Biosensors*, Birkhauser Verlag, Berlin (1989) 111.

133. Q.H. Gibson, B.E.P. Swoboda and V. Massay, *J. Biol. Chem*. 239 (1964) 3927-3934.

134. S. Nakamura, S. Hayashi and K. Koga, *Biochim. Biophys. Acta* 445 (1976) 294-308.

135. R. Seitz, T. Cole and J. Mullin, *11th Int. Congr. Clinical Chemistry*, Walter de Gruyter, Berlin, New York (1982) 1083.

136. M. Chen, W.P. Cai *et al*., *Anal. Chem. Acta* 388 (1999) 11-17.

137. T. Haruyama and M. Aizawa, *Biosensors and Bioelectron* 13 (1998) 1015-1022.

138. K. Sugawara, T. Takana *et al*., *Electroanal. Chem*. 482 (2000) 81-86.

139. Y. Shi and S.R. Crouch, *Anal. Chim. Acta* 381 (1999) 165-173.

140. C.R. Lowe and M.J. Goldfinch, *Biochem. Soc. Trans*. 11 (1983) 446.

141. W. Trettnak, M.J.P. Leiner and O. Wolfbeis, *Biosensors* 4 (1989) 15.

142. G. Nagy, L.H. Storp and G.G. Guilbault, *Anal.Chim Acta* 66 (1973) 443.

143. C. Tran-Minh and G. Broun, *Anal. Chem* 47 (1975) 1359.

144. G.G. Guilbault and G. Lubrano, *Anal. Chim Acta* 64 (1973) 439.

145. J.J. Kulys and N. Cenas, *Biochim Biophys. Acta* 744 (1983) 57.

146. P. Schlapfer, W. Mindt and P. Racine, *Clin. Chim. Acta* 57 (1974) 283.

147. A. Heller and Y. Degani, *J. Electrochem. Soc. Rev. News* 134 (1987) 494C.

148. Kazumichi Ban, Takeshi Ueki *et al*., *Electrochemical communications* 3 (2001) 649-653.

149. Kastis Krikstopaitis, Juozas Kulys and Lidija Tetianec, *Electrochemical communications* 6 (2004) 331-336.

150. D. Savitri, C.K. Mitra, *Biochem and Bioenerg*. 47 (1998) 67–73.

151. Gabriel ZoldáK, Anton Zubrik *et al*., *Journal of Biological Chem*. 279 (2004) 47601-47609.

152. P. Monsan, G. Puzo, and H. Marzarguil, *Biochimie* 57 (1975) 1281-1292.

PRESENTATIONS AND PUBLICATIONS

PRESENTATIONS

Poster presentations:

1. Electrochemical and Spectroscopic studies on dyes and proteins labeled with dyes

   B S B Salomi, C K Mitra and Lo Gorton

   6th International Topical Conference on Optical probes of Conjugated Polymers and Biosystems, Jan 4-8, 2005, Bangalore, India.

2. Electrocatalytic effect of redox dyes bound to Horseradish peroxidase
   B S B Salomi and C K Mitra

   International workshop on Biosensors for Environmental Analysis, Feb 21-23, 2006, Goa, India.

PUBLICATIONS

1. B.S.B. Salomi, C.K. Mitra and Lo Gorton, Electrochemistry of labeled proteins for biosensors, *Asian Journal of Physics*, Vol 14, (2005) 161-165.
2. B.S.B. Salomi, C.K. Mitra and Lo Gorton, Electrochemical and Spectroscopic studies on dyes and proteins labeled with dyes, Proceedings of the Sixth International Topical Conference on Optical Probes of Conjugated Polymers and Biosystems, *Synthetic metals* 155 (2005) 426-429.
3. B.S.B. Salomi and C.K. Mitra, Electrochemical studies on horseradish peroxidase covalently coupled with redox dyes, (*communicated*).
4. B.S.B. Salomi, Lo Gorton and C.K. Mitra, A promising electrochemical glucose biosensor based on electron transfer through redox dyes covalently coupled to glucose oxidase, (*communicated*).